Research Square

Preprints are preliminary reports that have not undergone peer review.
They should not be considered conclusive, used to inform clinical practice,
or referenced by the media as validated information.

Inhibition of Macrophage Senescence by Survivin Contributes to the Progression of Pulmonary Vascular Remodeling

Zhao Qixu
Capital Medical University
Sun Jiashu
Capital Medical University
Deng Yusong
Capital Medical University
Yao Zhizheng
Capital Medical University
Wu Huimin
Capital Medical University
Li Zhechen
Capital Medical University
Li Gang
angieligang@163.com
Capital Medical University

Article

Keywords: Pulmonary arterial hypertension, Survivin, Macrophage senescence, pulmonary vascular remodeling, Birc5

Posted Date: September 11th, 2026

DOI: https://doi.org/10.21203/rs.3.rs-10460683/v1

License: This work is licensed under a Creative Commons Attribution 4.0 International License.
Read Full License

Additional Declarations: No competing interests reported.

Abstract

Objective:

To investigate the role of Survivin in pulmonary vascular remodeling associated with pulmonary arterial hypertension (PAH) and elucidate whether it promotes pulmonary vascular remodeling by regulating macrophage senescence.

Methods:

An irreversible PAH model was established in Sprague-Dawley rats by left pneumonectomy plus subcutaneous monocrotaline. Rats received the Survivin inhibitor YM155 or vehicle.. Hemodynamics, right ventricular hypertrophy (Fulton index), and vascular remodeling (WT%) were assessed. Single-cell RNA sequencing (scRNA-seq) identified *Birc5* (Survivin) localization. *In vitro*, senescence was induced in NR8383 macrophages using doxorubicin. The effects of *Birc5* overexpression on macrophage senescence and the subsequent impact on pulmonary artery smooth muscle cell (PASMC) proliferation were evaluated using co-culture systems.

Results:

Survivin was significantly upregulated in PAH lungs. YM155 treatment reduced Survivin levels, improved hemodynamics, and attenuated remodeling, yet paradoxically increased senescence markers (SA-β-Gal, p16, γ-H2AX). scRNA-seq and immunofluorescence revealed that *Birc5* was primarily enriched in a macrophage subpopulation characterized by high expression of senescence genes. *In vitro*, *Birc5* overexpression significantly reversed doxorubicin-induced macrophage senescence (SA-β-Gal positive rate: 88.37% to 32.35%) and downregulated p16 and γ-H2AX. Notably, co-culture with senescent macrophages significantly inhibited PASMC proliferation, a protective effect partially abolished by Survivin.

Conclusion:

Survivin promotes pulmonary vascular remodeling in PAH by suppressing macrophage senescence. While inhibiting Survivin exerts therapeutic effects, it also induces a senescent macrophage phenotype that inhibits smooth muscle cell proliferation. These findings identify the Survivin–macrophage senescence axis as a novel mechanism and potential therapeutic target in PAH.

Introduction

Pulmonary arterial hypertension (PAH) is a progressive and frequently fatal cardiopulmonary disorder characterized by pulmonary vascular remodeling, elevated pulmonary vascular resistance, and eventual

right heart failure [1, 2].. Its pathological features include sustained vasoconstriction, medial thickening, intimal hyperplasia, inflammatory cell infiltration, and, in advanced disease, complex obstructive lesions [1–5]. Although targeted therapies such as endothelin receptor antagonists, prostacyclin analogues, and phosphodiesterase type 5 inhibitors have improved symptoms and prognosis in selected patients, these agents mainly modulate vasomotor tone and have limited efficacy against established structural remodeling [3–5]. Accordingly, further investigation into the molecular mechanisms driving pulmonary vascular remodeling remains of substantial scientific and clinical importance.

Survivin, encoded by BIRC5, is the smallest member of the inhibitor of apoptosis protein (IAP) family and plays key roles in mitosis, cell survival, and cell-cycle regulation [6–11].. Under physiological conditions, Survivin expression is low or undetectable in most differentiated adult tissues, whereas it is highly expressed in embryonic tissues and many malignancies [12–15]. Increased Survivin expression has been linked to enhanced proliferation, resistance to apoptosis, and adverse clinical outcomes in cancer [12–15].

Recent studies indicate that Survivin is also involved in pulmonary vascular disease[16, 17]. In addition, Survivin has been detected in lung tissue from patients with PAH, and pharmacological inhibition of Survivin has been reported to induce apoptosis in pulmonary artery smooth muscle cells (PASMCs), suppress their abnormal proliferation, and attenuate pulmonary vascular remodeling [16–18]. These observations suggest that Survivin acts as a promoting factor in PAH progression, however, most previous work has focused on PASMCs, and the cellular distribution of Survivin within the PAH lung, particularly in immune cells, remains incompletely defined.

Cellular senescence is a state of permanent cell cycle arrest traditionally viewed as a driver of age-related diseases. However, recent evidence suggests that it acts as a "double-edged sword" depending on the context of tissue repair and remodeling. In the context of PAH, the "SASP" (senescence-associated secretory phenotype) from various lung cells can influence neighboring cells. Interestingly, macrophages are primary orchestrators of the inflammatory milieu in PAH. Whether Survivin exerts its pro-remodeling effects by suppressing a protective senescent program in macrophages is a provocative but unexplored hypothesis.

In this study, we utilized a highly clinically relevant, irreversible rat model of PAH (Pneumonectomy + MCT) and single-cell RNA sequencing (scRNA-seq) to map the expression landscape of Birc5. We demonstrated that Survivin is predominantly enriched in macrophages during PAH progression. By inhibiting Survivin with YM155 and performing in vitro co-culture assays, we uncovered a novel mechanism: whereas senescent macrophages paradoxically serve as a brake on PASMC proliferation. This study provides a new perspective on the interplay between cell cycle regulation and immune cell function in PAH.

Materials and Methods

Animal Model of Pulmonary Arterial Hypertension

Thirty specific pathogen-free (SPF) male Sprague-Dawley rats, weighing 200–250 g, were purchased from Beijing HFK Bioscience Co., Ltd. (Beijing, China). All animals were housed under controlled conditions (temperature 20–25°C, humidity 50%–60%) with free access to food and water. Rats in the PAH and YM155 groups underwent left pneumonectomy under anesthesia induced by intraperitoneal injection of tribromoethanol (250 mg/kg). On postoperative day 7, irreversible PAH was induced by a subcutaneous injection of monocrotaline (MCT, 50 mg/kg). Rats in the YM155 group received intraperitoneal injections of the Survivin inhibitor YM155 (15 mg/kg) every other day starting from postoperative day 14, for a total of three doses. Rats in the control group (Con) underwent sham surgery and received vehicle injections at corresponding time points. Hemodynamic measurements and tissue collection were performed in all rats on postoperative day 28.

All experimental procedures were approved by the Ethics Committee of Beijing Anzhen Hospital, Capital Medical University (approval no. AZ2026LA023) and were conducted in accordance with relevant guidelines and regulations.

Hemodynamic Measurements and Tissue Processing

Right Ventricular Systolic Pressure Measurement: Rats were anesthetized with tribromoethanol (250 mg/kg, i.p.) and secured in a supine position. A puncture needle connected to a pressure transducer was inserted into the right ventricle approximately 0.5 cm above the point of maximal apical impulse, and right ventricular systolic pressure (RVSP) was recorded. Following the measurement, rats were euthanized by an intraperitoneal overdose of tribromoethanol while under deep anesthesia.

Assessment of Right Ventricular Hypertrophy: The heart was excised, and the right ventricle (RV) was carefully separated from the left ventricle plus septum (LV + S). Both portions were weighed, and the Fulton index (RV/[LV + S]) was calculated as an index of right ventricular hypertrophy.

Tissue Processing: The right middle lung lobe was fixed in 4% paraformaldehyde for 24 h, embedded in paraffin, and sectioned at a thickness of 5 μm for hematoxylin and eosin (HE) and elastica van Gieson (EVG) staining. The remaining lung tissue was snap-frozen in liquid nitrogen and stored at − 80°C for subsequent analyses.

Histological Staining and Morphometric Analysis

HE and EVG Staining: Staining was performed according to the manufacturer's instructions. Structural changes in pulmonary arterioles were observed under a light microscope and photographed.

Quantification of Pulmonary Vascular Remodeling:For each rat, five randomly selected pulmonary arterioles with diameters ranging from 50 to 100 μm were analyzed. Vessel wall thickness and lumen diameter were measured, and the percentage of wall thickness (WT%) was calculated using the formula: WT% = (2 × wall thickness / vessel diameter) × 100%.

Senescence-Associated β-Galactosidase (SA-β-Gal) Staining: Frozen lung sections (8 μm thickness) were stained using a senescence β-galactosidase staining kit according to the manufacturer's protocol. Sections were incubated overnight at 37°C, and blue-green positive cells were visualized under a microscope. For each group, five randomly selected fields were used to quantify the proportion of SA-β-Gal-positive cells.

Protein Extraction and Western Blotting

Protein Extraction: Lung tissue or cultured cells were homogenized or lysed in RIPA buffer supplemented with protease and phosphatase inhibitors on ice. The lysates were centrifuged at 12,000 g for 15 min at 4°C, and the supernatant was collected.

Protein Quantification: Protein concentrations were determined using the bicinchoninic acid (BCA) method.

Western Blotting: Equal amounts of protein were separated by SDS-PAGE and transferred onto polyvinylidene difluoride (PVDF) membranes (Millipore, 0.22 μm). Membranes were blocked with 5% non-fat milk for 1 h at room temperature and then incubated overnight at 4°C with primary antibodies against the following proteins: Survivin (1:1000, Abcam), p16 (1:2000, Thermo Fisher Scientific), γ-H2AX (1:1000, Cell Signaling Technology), and β-actin (1:10,000, Proteintech). After washing, membranes were incubated with horseradish peroxidase (HRP)-conjugated secondary antibodies (1:10,000, Proteintech) for 1 h at room temperature. Protein bands were visualized using an enhanced chemiluminescence (ECL) detection system, and band densities were quantified using ImageJ software.

Immunofluorescence

Paraffin-embedded lung sections were deparaffinized, subjected to antigen retrieval, and permeabilized with 0.1% Triton X-100 for 10 min. Following blocking with 5% normal goat serum for 30 min at room temperature, sections were incubated overnight at 4°C with primary antibodies against the following proteins: Survivin (1:300, Abcam, Cambridge, UK), CD68 (1:400, Abcam), and p16 (1:200, Thermo Fisher Scientific, Waltham, MA, USA). After washing, sections were incubated with fluorophore-conjugated secondary antibodies (1:400, Abcam) for 1 h at room temperature in the dark. Nuclei were counterstained with DAPI, and the sections were mounted. Fluorescence images were captured using a fluorescence microscope.

Cell Culture and Treatments

Cell Culture: The rat alveolar macrophage cell line NR8383 (Procell Life Science & Technology, Wuhan, China; Cat# CM-0172) was cultured in DMEM/F12 medium (Gibco, Thermo Fisher Scientific) supplemented with 15% fetal bovine serum (FBS; Gibco) and 1% penicillin/streptomycin (Procell). Primary rat pulmonary artery smooth muscle cells (PASMCs) were isolated and cultured in specialized complete medium (Procell; Cat# CM-R342). All cells were maintained at 37°C in a humidified incubator with 5% CO_2.

Induction of Senescence: NR8383 cells were treated with doxorubicin (0.2 μM; MedChemExpress, Monmouth Junction, NJ, USA) for 12 h. The medium was then replaced with fresh culture medium, and the cells were cultured for an additional 48 h to induce senescence.

Co-culture Experiments: Treated NR8383 cells were seeded into Transwell inserts (0.4 μm pore size; Corning, Corning, NY, USA). The inserts were placed into wells containing PASMCs, establishing a co-culture system. After 36 h of co-culture, PASMC proliferation was assessed.

Lentiviral Construction and Stable Transduction

Vector Construction: The rat Birc5 gene (encoding Survivin) was cloned into the pLVX-CMV-IRES-Puro lentiviral vector.

Virus Packaging: The recombinant plasmid was co-transfected into 293T cells with the packaging plasmid psPAX2 and the envelope plasmid pMD2.G using Lipofectamine 3000 (Thermo Fisher Scientific). Viral supernatants were collected at 48 h and 72 h post-transfection, filtered through 0.45 μm filters, and concentrated 100-fold by ultracentrifugation.

Titer Determination: Concentrated virus was serially diluted and used to infect 293T cells. The percentage of GFP-positive cells was determined by flow cytometry 72 h post-infection. The viral titer (TU/mL) was calculated using the formula: TU/mL = (number of positive cells × dilution factor × 10^4) / volume of viral supernatant.

Stable Transduction: NR8383 cells were transduced with the lentivirus at a multiplicity of infection (MOI) of 5 in the presence of polybrene (4 μg/mL). The medium was replaced 24 h post-transduction. At 48 h post-transduction, cells were subjected to selection with puromycin (2 μg/mL) for 7 days. Surviving cells were expanded, and Survivin overexpression was validated by Western blotting.

Cell Proliferation Assay (CCK-8)

PASMCs were seeded into 96-well plates at a density of 5,000 cells per well, with three replicate wells per experimental condition. Following the co-culture period, 10 μL of Cell Counting Kit-8 (CCK-8) reagent was added to each well, and the plates were incubated for 1 h at 37°C. Absorbance was measured at 450 nm using a microplate reader. Cell viability was expressed as the percentage of optical density (OD) values relative to the control group.

Statistical Analysis

All data are presented as the mean ± standard deviation (SD). Statistical analyses were performed using GraphPad Prism version 9.0 (GraphPad Software, San Diego, CA, USA). Comparisons among multiple groups were conducted using one-way or two-way analysis of variance (ANOVA), followed by Tukey's post hoc test for multiple comparisons. Comparisons between two groups were made using an unpaired

two-tailed Student's t-test or the Mann-Whitney U test (for data not normally distributed). A P-value < 0.05 was considered statistically significant.

Results

Combined Left Pneumonectomy and Monocrotaline Injection Induces Severe Pulmonary Arterial Hypertension in Rats

To evaluate the PAH model induced by left pneumonectomy combined with subcutaneous monocrotaline (MCT) injection and to investigate the therapeutic effects of the Survivin inhibitor YM155, we assessed the general condition and survival of rats in each group, and measured hemodynamic parameters and indicators of right ventricular remodeling.

Compared with the healthy control group (Con), rats in the PAH model group exhibited characteristic behavioral changes, including tachypnea, reduced appetite, and decreased activity tolerance. Hemodynamic analysis revealed that right ventricular systolic pressure (RVSP) was significantly elevated in the PAH group compared to the Con group (Fig. 1A, $P < 0.05$). Treatment with the Survivin inhibitor YM155 significantly attenuated this increase in RVSP ($P < 0.05$). The Fulton index [RV/(LV + S)], an indicator of right ventricular hypertrophy that indirectly reflects the extent of pulmonary vascular remodeling, was significantly higher in the PAH group than in the other two groups (Fig. 1B, $P < 0.05$). Additionally, rats in the PAH group exhibited lower body weight (Fig. 1C, $P < 0.05$) and higher mortality (Fig. 1D) compared to the Con and YM155-treated groups. Administration of YM155 effectively reduced RVSP and the Fulton index in PAH rats and markedly improved their survival rate.

To directly assess whether left pneumonectomy combined with MCT injection induces pulmonary vascular remodeling and to evaluate the impact of YM155 intervention, we performed hematoxylin and eosin (HE) and elastica van Gieson (EVG) staining on lung tissue sections. Histopathological examination revealed that pulmonary arterioles from PAH rats exhibited marked luminal stenosis, occlusion, and vascular remodeling, accompanied by substantial inflammatory cell infiltration. In contrast, these pathological changes were less severe in the YM155 intervention group (Fig. 1E, F). Quantitative analysis of pulmonary vascular remodeling was performed by randomly selecting five pulmonary arterioles per rat and calculating the percentage of wall thickness (WT% = 2 × wall thickness / vessel diameter × 100%). The WT% was significantly higher in the PAH group compared to the Con group (Fig. 1G, $P < 0.05$), confirming the presence of irreversible pulmonary vascular remodeling. YM155 treatment significantly reduced the WT% compared to the untreated PAH group ($P < 0.05$).

Collectively, these results demonstrate that combined left pneumonectomy and MCT injection successfully induces severe PAH accompanied by irreversible pulmonary vascular remodeling. The Survivin inhibitor YM155 attenuates these pathological changes, suggesting that Survivin promotes PAH progression and that pharmacological inhibition of Survivin exerts therapeutic effects in this model.

Survivin Expression is Upregulated in the Lungs of PAH Rats and Suppressed by YM155

To investigate the expression pattern of Survivin during the pathogenesis of PAH and its relationship with the therapeutic effects of YM155, we examined Survivin protein levels in lung tissues from each group using Western blotting. As shown in Fig. 2A, B, Survivin protein expression was significantly elevated in the PAH group compared to the Con group ($P < 0.05$). Administration of the Survivin-specific inhibitor YM155 markedly reduced Survivin expression compared to the untreated PAH group ($P < 0.05$). These results indicate that the progression of PAH is accompanied by upregulation of Survivin protein, and that YM155 effectively suppresses this increase.

To further validate the cellular localization and distribution of Survivin expression within the lung tissue, we performed immunofluorescence staining on lung sections from each group. Consistent with the Western blot findings, immunofluorescence analysis revealed strong Survivin fluorescence signals (red) in the PAH group, which were widely distributed and primarily localized to the pulmonary vessel walls and some perialveolar cells (Fig. 2C). In contrast, Survivin fluorescence was substantially weaker in the YM155-treated group, and nearly undetectable in the Con group.

Taken together with our previous findings, these results demonstrate that Survivin is highly expressed in the lungs of PAH rats and plays a significant role in disease progression. As a specific inhibitor of Survivin, YM155 downregulates Survivin expression at the protein level, which likely contributes to its ameliorative effects on pulmonary vascular remodeling.

Inhibition of Survivin exacerbates the cellular senescence phenotype in PAH lung tissue.

To assess the overall impact of Survivin inhibition on cellular senescence in the PAH model, we performed SA-β-Gal staining on lung tissue and quantified the proportion of positive cells (Figure A). As shown in Figure A, the control group exhibited normal lung tissue structure with almost no SA-β-Gal-positive cells (blue-green). In the PAH group, the number of positively stained cells (blue-green) was significantly increased, indicating that the PAH disease model itself is accompanied by the activation of cellular senescence. Notably, the YM155 group displayed the highest number of blue-positive cells and the most intense staining in lung tissue, significantly exceeding that of the PAH group. This suggests that Survivin exerts an inhibitory effect on senescence in the context of PAH. Quantitative analysis of the positively stained area confirmed these observations: SA-β-Gal activity was significantly higher in the PAH group than in the Con group, and activity in the YM155 group was further elevated compared to the PAH group .

Next, to validate the above phenotype at the molecular level, we examined the expression levels of p16INK4a (CDKN2A), a key regulator of cellular senescence, and γ-H2AX, a marker of DNA damage, by Western blot (Figures C, D, E, F). The Western blot results were consistent with the SA-β-Gal findings. Compared with the Con group, the levels of p16INK4a and γ-H2AX in lung tissue were significantly

upregulated in the PAH group. Furthermore, YM155 treatment significantly enhanced the expression of both proteins ($p < 0.05$).

These results indicate that while pulmonary arterial hypertension (PAH) itself induces cellular senescence and DNA damage, inhibiting Survivin function exacerbates this process. This suggests that cellular senescence may play a protective role in the pathological progression of PAH, and the elevated expression of these markers might represent an adaptive response of cells to stress. By suppressing cellular senescence, Survivin may further contribute to the progression of pulmonary arterial hypertension.

Single-cell RNA sequencing reveals enrichment of Survivin in senescence-associated macrophages

To unbiasedly identify the key cell types involved in the pathological process of pulmonary arterial hypertension (PAH), particularly those associated with cellular senescence-related molecular events, we performed high-throughput single-cell RNA sequencing (scRNA-seq) on lung tissue. Following rigorous quality control (including the exclusion of low-quality cells, cells with high mitochondrial gene content, and doublets) and standardized data processing, we obtained high-quality transcriptomic data from 10,000 single cells.

Through unsupervised clustering analysis based on gene expression profiles and subsequent cell annotation using canonical cell type-specific markers, we successfully identified the major cell types in the lung, including alveolar epithelial cells, endothelial cells, fibroblasts, smooth muscle cells, T cells, and macrophages. To precisely delineate the expression distribution of Survivin across the lung cellular landscape, its encoding gene Birc5 was visualized on the cellular atlas (Figure A, B). Notably, the upregulation of Birc5 expression in the PAH context was not widespread but was predominantly enriched within a specific subset of macrophages ($CD68^+$, $CD14^+$ markers) (Figure C). This scRNA-seq finding was independently validated at the protein spatial distribution level by subsequent co-immunostaining for CD68 (a macrophage marker) and Survivin, confirming the specific high expression of Survivin in lung macrophages under PAH conditions.

Furthermore, within the macrophage subpopulation exhibiting high Birc5 expression, the expression levels of several canonical markers associated with cellular senescence and DNA damage were concurrently altered. Specifically, the expression levels of the senescence markers Cdkn2a (p16) and Cdkn1a (p21), as well as the DNA damage marker H2afx (γ-H2AX), were also upregulated (Figure A, B). Additionally, KEGG enrichment analysis of the top 50 upregulated genes in the PAH group revealed significant enrichment of pathways related to cellular senescence and the cell cycle, providing pathway-level evidence for the widespread activation of cellular senescence in PAH (Figure D, E).

To validate these bioinformatic findings in situ at the tissue level, we performed CD68 and p16 co-immunofluorescence staining on rat lung tissue sections. The results demonstrated that, compared to

the Con group, the PAH group exhibited markedly elevated p16 expression signals, which colocalized with CD68-labeled macrophages (Figure F). This visually confirms the macrophage senescence phenotype. Notably, the YM155 group displayed even higher p16 expression levels, further corroborating our conclusions from another perspective.

Overexpression of Survivin Inhibits Doxorubicin-Induced Macrophage Senescence

To further elucidate the effect of Survivin on senescent macrophages, we established a NR8383 rat macrophage cell line stably overexpressing Birc5, the gene encoding Survivin. A recombinant lentiviral vector carrying the Birc5 gene, along with a GFP reporter gene and a puromycin resistance gene for subsequent cell selection, was constructed. NR8383 cells were transduced with the recombinant lentivirus at a multiplicity of infection (MOI) of 5 (NR8383-Birc5-OE), a titer predetermined through preliminary experiments to ensure high transfection efficiency with minimal cytotoxicity. NR8383 cells transduced with empty lentivirus (NR8383-NC) and untransduced NR8383 cells (NR8383-WT) served as controls. At 48 hours post-transduction, obvious green fluorescence signals were observed under a fluorescence microscope in the NR8383-Birc5-OE and NR8383-NC groups, while no fluorescence was detected in the NR8383-WT group (Figure A). Counting in random fields confirmed successful transduction in the vast majority of cells. Subsequently, the transduced cells were continuously selected using DMEM/F12 medium containing 2.0 μg/mL puromycin to ensure the acquisition of macrophages stably expressing the target gene.

To evaluate the effectiveness of puromycin selection and confirm the successful establishment of stable transgenic cell lines, we monitored the viability of cells from each group over four consecutive days using the CCK-8 assay (Figure B). As shown, the viability of NR8383-WT cells decreased sharply within three days of puromycin treatment and reached a minimum by day 4, indicating that the selection concentration was effective and sufficient to kill all untransduced cells. In contrast, although the viability of NR8383-NC and NR8383-Birc5-OE cells transiently decreased during the initial selection period (days 1–2), it subsequently recovered rapidly, and the cells continued to proliferate. These results demonstrate that the lentivirus carrying the puromycin resistance gene was successfully integrated into the cell genome and conferred resistance. To confirm stable expression of the Survivin protein encoded by the Birc5 gene in macrophages, Western blot analysis was performed. The results showed that Survivin protein expression levels were significantly increased in the NR8383-Birc5-OE group, whereas no Survivin expression was detected in the control groups (Figure C).

To verify the effect of Survivin on cellular senescence, we established a cellular senescence model using doxorubicin and identified senescent cells by SA-β-Gal staining (Figure D). As shown in Figure D, no senescent cells were observed in the two groups not treated with doxorubicin. In the NR8383-Sen group treated with doxorubicin, a large number of SA-β-Gal-positive cells were observed, exhibiting the morphological characteristics of senescent cells. Importantly, in the NR8383-Birc5-OE + Sen group, which was also treated with doxorubicin, the proportion of SA-β-Gal-positive cells was significantly lower

than that in the NR8383-Sen group. Statistical analysis of the SA-β-Gal-positive cell rate revealed that the positive rate was 88.37% in the NR8383-Sen group, which decreased to 32.35% in the NR8383-Birc5-OE + Sen group. These results indicate that doxorubicin successfully induced macrophage senescence, and Survivin overexpression significantly inhibited this process by reducing the proportion of senescent cells.

DNA damage, as an initiating event in cellular senescence, activates downstream signaling pathways that lead to senescence. Therefore, the DNA damage marker γ-H2AX can also serve as an indicator of cellular senescence. Western blot analysis showed that γ-H2AX expression levels were markedly elevated in the NR8383-Sen group, while expression levels in the NR8383-Birc5-OE + Sen group were lower compared to the NR8383-Sen group (Figure E). This suggests that Survivin inhibits cellular senescence, consistent with its known role in promoting cell proliferation. Similarly, Western blot analysis of the cellular senescence marker p16 revealed that its expression was upregulated in doxorubicin-induced senescent macrophages, but this upregulation was significantly attenuated in doxorubicin-induced macrophages overexpressing Birc5 (Figure E).

During the pathogenesis and progression of pulmonary arterial hypertension, the proliferation and migration of pulmonary arterial smooth muscle cells (PASMCs) play a critical role. To investigate the effect of senescent macrophages on PASMCs, we performed co-culture experiments using Transwell chambers. The experiment was divided into four groups: PASMCs co-cultured with NR8383-WT cells, NR8383-Birc5-OE cells, senescent NR8383 cells (NR8383-Sen), and senescent NR8383 cells overexpressing Birc5 (NR8383-Birc5-OE-Sen). PASMC proliferation was assessed using the CCK-8 assay. The results showed that in the co-culture system, PASMC proliferation was significantly decreased in the senescence group compared to the NC group, suggesting that senescent macrophages influence PASMC proliferation through certain mechanisms. Notably, Survivin overexpression in macrophages partially counteracted this inhibitory effect (Figure F).

Discussion

This study systematically investigated the role of Survivin in pulmonary vascular remodeling associated with pulmonary arterial hypertension (PAH) and its underlying regulatory mechanisms by integrating animal models, single-cell RNA sequencing, and in vitro experiments. An irreversible PAH rat model was established using left pneumonectomy combined with subcutaneous injection of monocrotaline. Model animals exhibited typical pathophysiological features of PAH, including significantly elevated right ventricular systolic pressure (RVSP), increased right ventricular hypertrophy, and pulmonary arteriolar stenosis/occlusion. Intervention with the Survivin inhibitor YM155 significantly ameliorated these parameters, suggesting that Survivin plays a promoting role in PAH progression. Paradoxically, YM155 treatment led to an increase in cellular senescence-associated indicators, implying that Survivin suppresses cellular senescence. Single-cell RNA sequencing, along with subsequent experiments, revealed that Survivin is expressed in a macrophage subpopulation that exhibits a senescent phenotype in the context of PAH. In vitro studies confirmed that overexpression of Survivin inhibited doxorubicin-induced macrophage senescence and reduced the expression of senescence-associated markers.

The Role of Survivin in Pulmonary Vascular Remodeling

Left pneumonectomy, by drastically reducing the pulmonary vascular bed capacity, substantially increases blood flow and shear stress in the remaining right lung vasculature. This abnormal mechanical stress activates endothelial cells, initiating pro-inflammatory and pro-proliferative signaling pathways[24]. Concurrently, the remaining pulmonary vasculature undergoes compensatory hyperplasia, collectively exacerbating the pulmonary vascular remodeling process[24]. Monocrotaline itself is a non-toxic pyrrolizidine alkaloid; however, upon metabolic conversion by hepatic cytochrome P450 enzymes into highly reactive pyrrole derivatives, it reaches the lungs via the circulation and induces endothelial cell injury[25]. While monocrotaline injection alone can induce PAH, some models exhibit reversibility over time. Pneumonectomy alone typically results in only mild PAH and vascular remodeling. The abnormally elevated shear stress following left pneumonectomy not only directly promotes pulmonary vascular remodeling but also renders endothelial cells more susceptible to monocrotaline-induced damage. Concurrently, the endothelial injury and inflammation caused by monocrotaline are rapidly exacerbated under the impact of high blood flow, triggering a more pronounced proliferative response. Therefore, the combination of left pneumonectomy and monocrotaline injection induces a more severe and irreversible form of PAH.

Accumulating evidence indicates that Survivin plays a critical pathogenic role in PAH. Survivin is overexpressed in the pulmonary vasculature of PAH patients and animal models, where it promotes resistance to apoptosis and drives aberrant proliferation of pulmonary artery smooth muscle cells (PASMCs)[16–18]. Beyond PASMCs, our single-cell RNA sequencing data reveal that Survivin is also highly expressed in a subset of lung macrophages under PAH conditions, suggesting a broader cellular impact. YM155, a specific inhibitor of Survivin, potently suppresses Survivin expression by binding to transcriptional regulatory proteins such as ILF3[26]. In our study, YM155 treatment significantly attenuated the PAH phenotype, confirming Survivin as a disease-promoting factor. Notably, YM155 simultaneously upregulated cellular senescence markers, suggesting that Survivin suppresses senescence in the PAH lung. This raises the possibility that Survivin contributes to PAH progression not only by promoting cell survival and proliferation but also by actively inhibiting protective senescence programs. Thus, the combination of left pneumonectomy and monocrotaline injection provides a relevant model to study this Survivin–senescence axis in irreversible pulmonary vascular remodeling.

Macrophage Senescence: A Potential Protective Mechanism

Current evidence suggests that cellular senescence exerts a "double-edged sword" effect in pathophysiology. The detrimental role of cellular senescence in disease progression has been demonstrated in various models, including neurodegenerative diseases and osteoarthritis[27–29]. On one hand, senescent cells withdraw from the cell cycle and exhibit functional decline, directly contributing to organ dysfunction. On the other hand, pro-inflammatory factors within the senescence-associated secretory phenotype (SASP) establish a chronic local inflammatory state, interfering with the normal function of neighboring cells and inducing paracrine effects that indirectly promote disease progression

[27–29]. Conversely, other studies have indicated that cellular senescence can exert protective effects by inhibiting cell proliferation, promoting inflammation resolution, and facilitating immune clearance [30–33]. In the present study, the increased cellular senescence induced by the Survivin inhibitor YM155 may represent a compensatory mechanism in response to PAH. By promoting the senescence of key cells such as macrophages, this mechanism could limit their hyperactivation and the release of associated SASP factors, thereby restricting the impact of senescent cells on the surrounding microenvironment and modulating the senescent niche to inhibit pulmonary vascular remodeling. This notion is supported by our experimental findings: although senescence-associated m155 treatment, PAH indicators (such as RVSP, right ventricular hypertrophy, and pulmonary vascular remodeling) were alleviated.Previous studies have demonstrated that the accumulation of pro-inflammatory cytokines such as IL-6, IL-1β, and TNF-α—key components of the senescence-associated secretory phenotype (SASP)—plays a critical role in initiating paracrine senescence. These factors activate conserved senescence signaling pathways within recipient cells by engaging their cognate receptors (IL-1R, TNFR). Specifically, IL-1α/β often serve as upstream triggers, activating the transcription factors NF-κB and C/EBPβ, which in turn drive a “SASP amplification loop” in recipient cells, whereby non-senescent cells begin to express SASP-related genes upon stimulation. This positive feedback mechanism enables the propagation of senescence signals in a cascading manner across the cell population. In addition, members of the TGF-β family exert dual roles in SASP-mediated paracrine senescence: in the early stages of senescence or in specific cell types, TGF-β directly inhibits the proliferation of neighboring cells and induces cell cycle arrest by upregulating p15 and p21, thereby promoting the establishment of a senescent phenotype[34].

The Paracrine Influence: SASP and the Microenvironment

This study establishes a link between Survivin, PAH, and cellular senescence, offering a novel framework for understanding PAH pathogenesis. While the Survivin inhibitor YM155 has been explored in oncology, its therapeutic potential in PAH remains largely unknown. Our study provides preclinical evidence that YM155 ameliorates PAH in an animal model. Our findings suggest that YM155 may alleviate PAH through a dual mechanism: directly inhibiting Survivin's pro-proliferative and anti-apoptotic effects in pulmonary vascular cells, and indirectly promoting macrophage senescence, which in turn modulates the senescence-associated secretory phenotype (SASP) and limits local inflammation. Furthermore, our single-cell data indicate that Survivin is enriched in a subpopulation of macrophages where senescence markers are also upregulated upon YM155 treatment, suggesting that these cells may serve as key mediators of the therapeutic response. Together, these results provide a rationale for targeting Survivin in PAH therapy, potentially offering an approach distinct from current vasodilator-based treatments. Additionally, Survivin and cellular senescence markers such as p16 and γ-H2AX hold potential as novel biomarkers for reflecting PAH severity and monitoring treatment response.

Clinical Implications and Limitations

This study has several limitations. First, the findings are based solely on animal and cellular models and lack validation in human samples. Second, although this study identified that Survivin modulates

pulmonary vascular remodeling by inhibiting macrophage senescence, the specific downstream signaling pathways remain to be elucidated. Third, the molecular mechanisms through which senescent macrophages influence surrounding cells (pulmonary artery endothelial cells and smooth muscle cells) require further investigation. Future research should focus on delineating the precise signaling networks by which Survivin regulates macrophage senescence and exploring strategies to modulate senescence programs in specific cell types, rather than globally, to achieve safer and more effective therapeutic interventions for PAH.

In conclusion, our data indicate that Survivin is upregulated in lung macrophages in experimental PAH and is associated with reduced macrophage senescence. YM155 treatment attenuated pulmonary vascular remodeling while increasing senescence-associated markers, suggesting that modulation of macrophage senescence may contribute to the observed therapeutic effect. Further studies are needed to establish cell-specific causality and define the downstream signaling mechanisms.

Declarations

Conflict of Interest Statement

The authors declare that there is no conflict of interest regarding the publication of this paper. No financial or personal relationships have influenced the work reported in this manuscript.

Funding

The authors disclosed receipt of the following financial support for the research, authorship, and/or publication of this article: This work was supported by the Beijing Natural Science Foundation [Grant Number L258027].

Author Contribution

All authors contributed to the study conception and design. The experiments, data collection and analysis were performed by Zhao Qixu, Sun Jiashu , Deng Yusong Yao Zhizheng,Wu Huimin and Li Zhechen . The experimental design and funding were provided by Li Gang.The first draft of the manuscript was written by Zhao Qixu and all authors commented on previous versions of the manuscript. All authors read and approved the final manuscript.

Data Availability

The single-cell RNA-sequencing datasets generated in this study are publicly available in the NCBI Gene Expression Omnibus (GEO) under accession number GSE344118

(https://www.ncbi.nlm.nih.gov/geo/query/acc.cgi?acc=GSE344118).

Declaration of Conflicting Interests

The authors declared no potential conflicts of interest with respect to the research, authorship, and/or publication of this article.

References

1. Fazal, S., Bisserier, M. & Hadri, L. Molecular and Genetic Profiling for Precision Medicines in Pulmonary Arterial Hypertension. *Cells* **10** (3), 638 (2021).
2. Naeije, R., Richter, M. J. & Rubin, L. J. The physiological basis of pulmonary arterial hypertension. *Eur. Respir J.* **59** (6), 2102334 (2022).
3. Ruopp, N. F. & Cockrill, B. A. Diagnosis and Treatment of Pulmonary Arterial Hypertension: A Review. *JAMA* **327** (14), 1379–1391 (2022).
4. Liu, R. et al. Insights into Endothelin Receptors in Pulmonary Hypertension. *Int. J. Mol. Sci.* **24** (12), 10206 (2023).
5. Hoeper, M. M. et al. A global view of pulmonary hypertension. *Lancet Respir Med.* **4** (4), 306–322 (2016).
6. Wheatley, S. P. The functional repertoire of survivin's tails. *Cell. Cycle*. **14** (2), 261–268 (2015).
7. Altieri, D. C. Survivin in apoptosis control and cell cycle regulation in cancer. *Prog Cell. Cycle Res.* **5**, 447–452 (2003).
8. Li, F. et al. Control of apoptosis and mitotic spindle checkpoint by survivin. *Nature* **396** (6711), 580–584 (1998).
9. Vagnarelli, P. & Earnshaw, W. C. Chromosomal passengers: the four-dimensional regulation of mitotic events. *Chromosoma* **113** (5), 211–222 (2004).
10. Wheatley, S. P. & McNeish, I. A. Survivin: a protein with dual roles in mitosis and apoptosis. *Int. Rev. Cytol.* **247**, 35–88 (2005).
11. Chi, Y. et al. Survivin-targeting Artificial MicroRNAs Mediated by Adenovirus Suppress Tumor Activity in Cancer Cells and Xenograft Models. *Mol. Ther. Nucleic Acids*. **3** (11), e208 (2014).
12. Shintani, M. et al. Immunohistochemical expression of nuclear and cytoplasmic survivin in gastrointestinal carcinoma. *Int. J. Clin. Exp. Pathol.* **6** (12), 2919–2927 (2013).
13. Kim, Y. H. et al. Evaluation of survivin as a prognostic marker in oral squamous cell carcinoma. *J. Oral Pathol. Med.* **39** (5), 368–375 (2010).
14. Nigam, J. et al. Expression of survivin mRNA in gallbladder cancer: a diagnostic and prognostic marker? *Tumour Biol.* **35** (9), 9241–9246 (2014).
15. Lu, C. D., Altieri, D. C. & Tanigawa, N. Expression of a novel antiapoptosis gene, survivin, correlated with tumor cell apoptosis and p53 accumulation in gastric carcinomas. *Cancer Res.* **58** (9), 1808–

1812 (1998).

16. Li, G. et al. The expression of survivin in irreversible pulmonary arterial hypertension rats and its value in evaluating the reversibility of pulmonary arterial hypertension secondary to congenital heart disease. *Pulm Circ.* **9** (3), 2045894019859480 (2019).
17. Ye, B. et al. Effects of YM155 on the proliferation and apoptosis of pulmonary artery smooth muscle cells in a rat model of high pulmonary blood flow-induced pulmonary arterial hypertension. *Clin. Exp. Hypertens.* **44** (5), 470–479 (2022).
18. McMurtry, M. S. et al. Gene therapy targeting survivin selectively induces pulmonary vascular apoptosis and reverses pulmonary arterial hypertension. *J. Clin. Invest.* **115** (6), 1479–1491 (2005).
19. Wang, B. et al. The senescence-associated secretory phenotype and its physiological and pathological implications. *Nat. Rev. Mol. Cell. Biol.* **25** (12), 958–978 (2024).
20. Langhi Prata, L. G. P., Tchkonia, T. & Kirkland, J. L. Cell senescence, the senescence-associated secretory phenotype, and cancers. *PLoS Biol.* **21** (9), e3002326 (2023).
21. Mebratu, Y. A. et al. The aged extracellular matrix and the profibrotic role of senescence-associated secretory phenotype. *Am. J. Physiol. Cell. Physiol.* **325** (3), C565–C579 (2023).
22. Cen, P. et al. Cellular senescence imaging and senolysis monitoring in cancer therapy based on a β-galactosidase-activated aggregation-induced emission luminogen. *Acta Biomater.* **179**, 340–353 (2024).
23. Sharma, S. et al. Survivin inhibition ameliorates liver fibrosis by inducing hepatic stellate cell senescence and depleting hepatic macrophage population. *J. Cell. Commun. Signal.* **18** (1), e12015 (2024).
24. Tsikis, S. T. et al. A pneumonectomy model to study flow-induced pulmonary hypertension and compensatory lung growth. *Cell. Rep. Methods*. **3** (10), 100613 (2023).
25. Wilson, D. W. et al. Mechanisms and pathology of monocrotaline pulmonary toxicity. *Crit. Rev. Toxicol.* **22** (5–6), 307–325 (1992).
26. Başpınar, Y. et al. Development and characterization of nanobubbles containing paclitaxel and survivin inhibitor YM155 against lung cancer. *Int. J. Pharm.* **566**, 149–156 (2019).
27. Si, Z., Sun, L. & Wang, X. Evidence and perspectives of cell senescence in neurodegenerative diseases. *Biomed. Pharmacother*. **137**, 111327 (2021).
28. Saez-Atienzar, S. & Masliah, E. Cellular senescence and Alzheimer disease: the egg and the chicken scenario. *Nat. Rev. Neurosci.* **21** (8), 433–444 (2020).
29. Chen, X. et al. METTL3-mediated m6A modification of ATG7 regulates autophagy-GATA4 axis to promote cellular senescence and osteoarthritis progression. *Ann. Rheum. Dis.* **81** (1), 87–99 (2022).
30. Muñoz-Espín, D. et al. Programmed cell senescence during mammalian embryonic development. *Cell* **155** (5), 1104–1118 (2013).
31. Storer, M. et al. Senescence is a developmental mechanism that contributes to embryonic growth and patterning. *Cell* **155** (5), 1119–1130 (2013).

32. Demaria, M. et al. An essential role for senescent cells in optimal wound healing through secretion of PDGF-AA. *Dev. Cell.* **31** (6), 722–733 (2014).
33. Krizhanovsky, V. et al. Senescence of activated stellate cells limits liver fibrosis. *Cell* **134** (4), 657–667 (2008).
34. Acosta, J. C. et al. A complex secretory program orchestrated by the inflammasome controls paracrine senescence. *Nat. Cell. Biol.* **15** (8), 978–990 (2013).

Figures

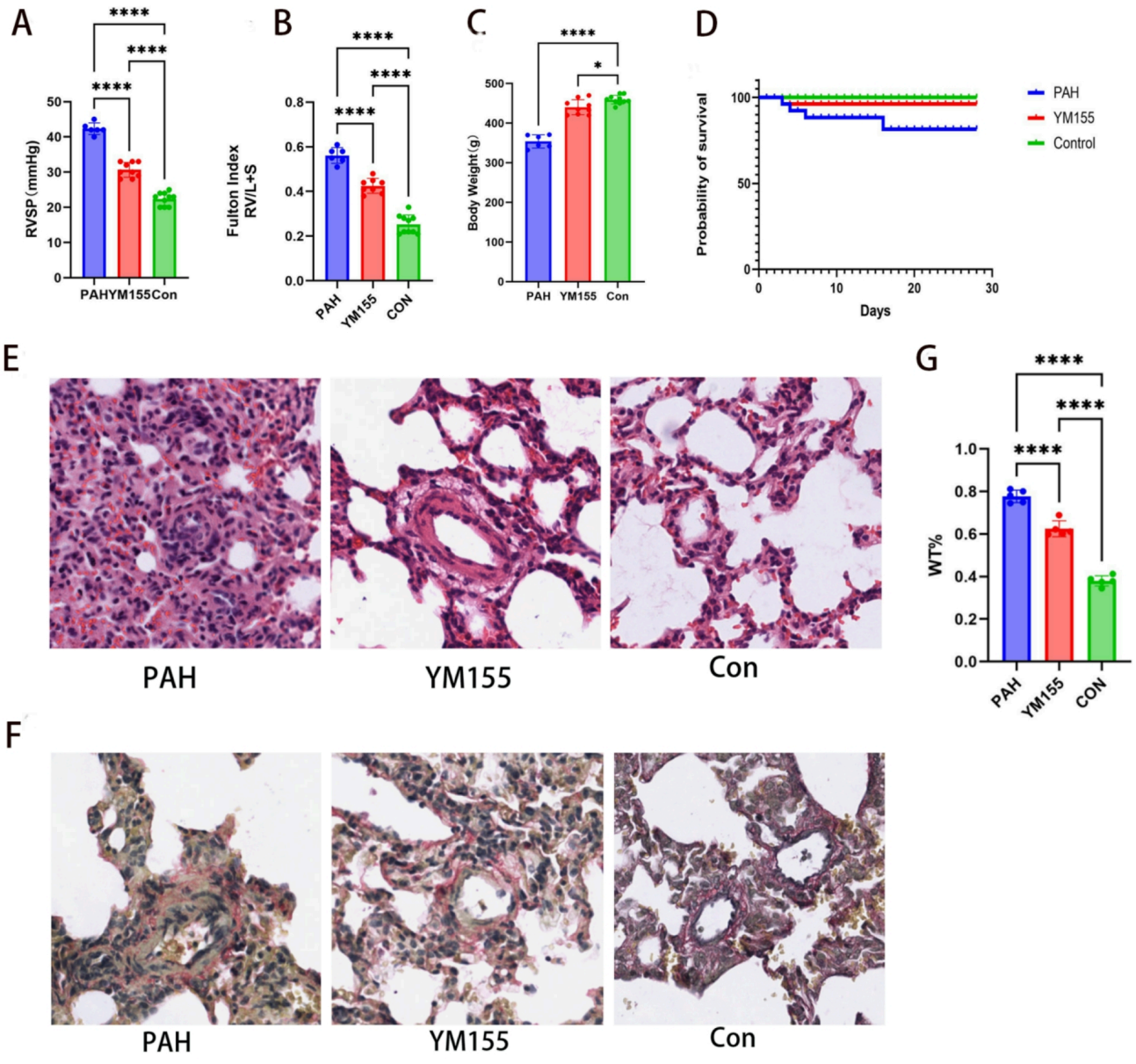

Figure 1

Effect of Survivin on RVSP, Right Ventricular Hypertrophy, Body Weight, and Survival Rate in Rats. (A) Quantitative analysis of right ventricular systolic pressure (RVSP) measured by transthoracic right ventricular puncture. (B) Quantitative analysis of right ventricular hypertrophy assessed by the Fulton index [RV/(LV+S)]. (C) Quantitative analysis of rat body weight at the time of tissue collection. (D) Kaplan-Meier survival curves for rats in each group. (E) Representative images of hematoxylin and eosin (HE) staining showing pulmonary histopathology. (F) Representative images of elastica van Gieson (EVG) staining showing pulmonary vascular structure. (G) Quantitative analysis of the percentage of pulmonary arteriolar wall thickness (WT%). PAH: pulmonary arterial hypertension model group; YM155: YM155 intervention group; Con: control group. Data are presented as mean ± SD (n = 10 per group). *P < 0.05.

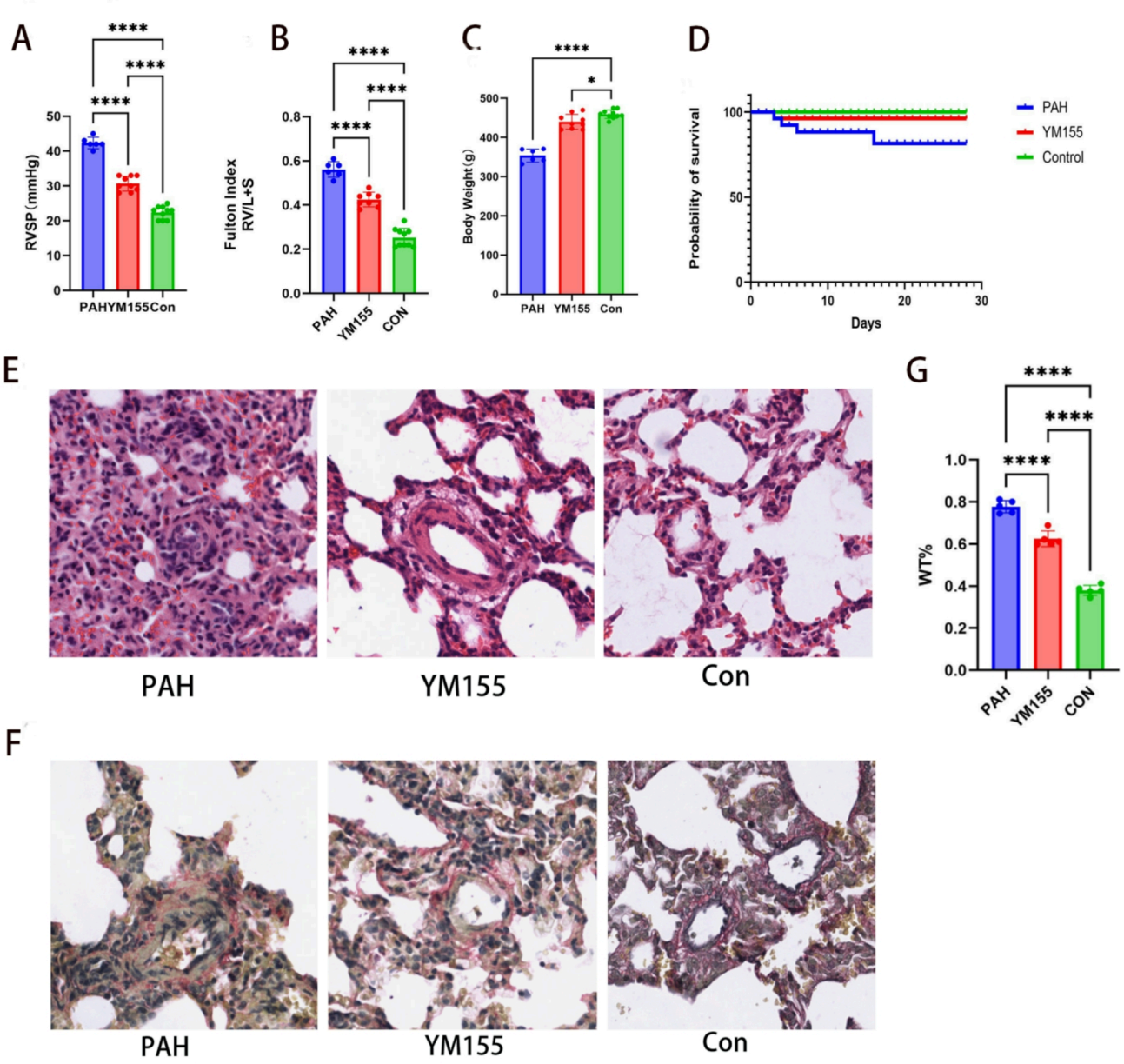

Figure 1

Effect of Survivin on RVSP, Right Ventricular Hypertrophy, Body Weight, and Survival Rate in Rats. (A) Quantitative analysis of right ventricular systolic pressure (RVSP) measured by transthoracic right ventricular puncture. (B) Quantitative analysis of right ventricular hypertrophy assessed by the Fulton index [RV/(LV+S)]. (C) Quantitative analysis of rat body weight at the time of tissue collection. (D) Kaplan-Meier survival curves for rats in each group. (E) Representative images of hematoxylin and eosin (HE) staining showing pulmonary histopathology. (F) Representative images of elastica van Gieson (EVG) staining showing pulmonary vascular structure. (G) Quantitative analysis of the percentage of pulmonary arteriolar wall thickness (WT%). PAH: pulmonary arterial hypertension model group; YM155: YM155 intervention group; Con: control group. Data are presented as mean ± SD (n = 10 per group). *P < 0.05.

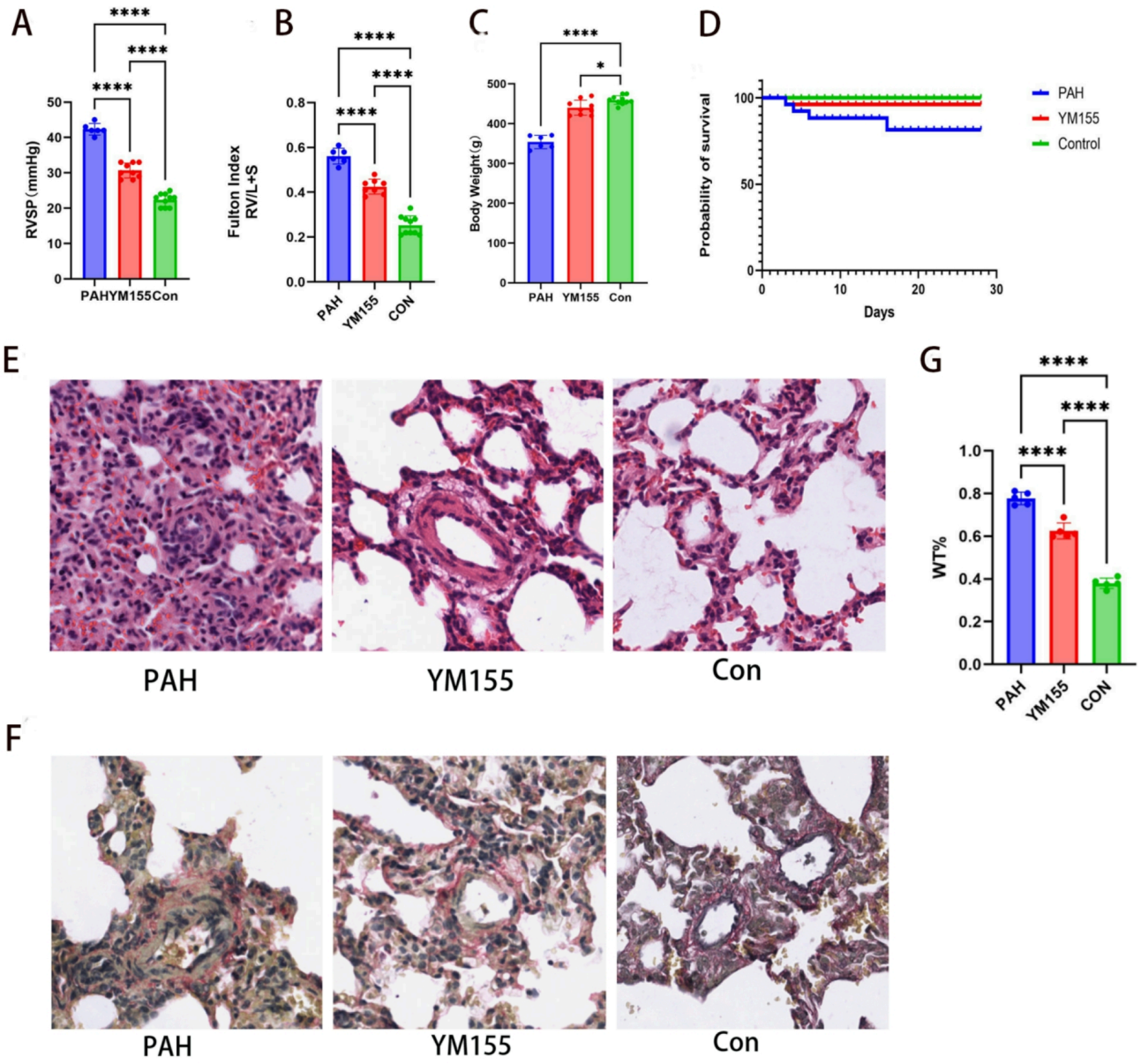

Figure 1

Effect of Survivin on RVSP, Right Ventricular Hypertrophy, Body Weight, and Survival Rate in Rats. (A) Quantitative analysis of right ventricular systolic pressure (RVSP) measured by transthoracic right ventricular puncture. (B) Quantitative analysis of right ventricular hypertrophy assessed by the Fulton index [RV/(LV+S)]. (C) Quantitative analysis of rat body weight at the time of tissue collection. (D) Kaplan-Meier survival curves for rats in each group. (E) Representative images of hematoxylin and eosin (HE) staining showing pulmonary histopathology. (F) Representative images of elastica van Gieson (EVG) staining showing pulmonary vascular structure. (G) Quantitative analysis of the percentage of pulmonary arteriolar wall thickness (WT%). PAH: pulmonary arterial hypertension model group; YM155:

YM155 intervention group; Con: control group. Data are presented as mean ± SD (n = 10 per group). *P < 0.05.

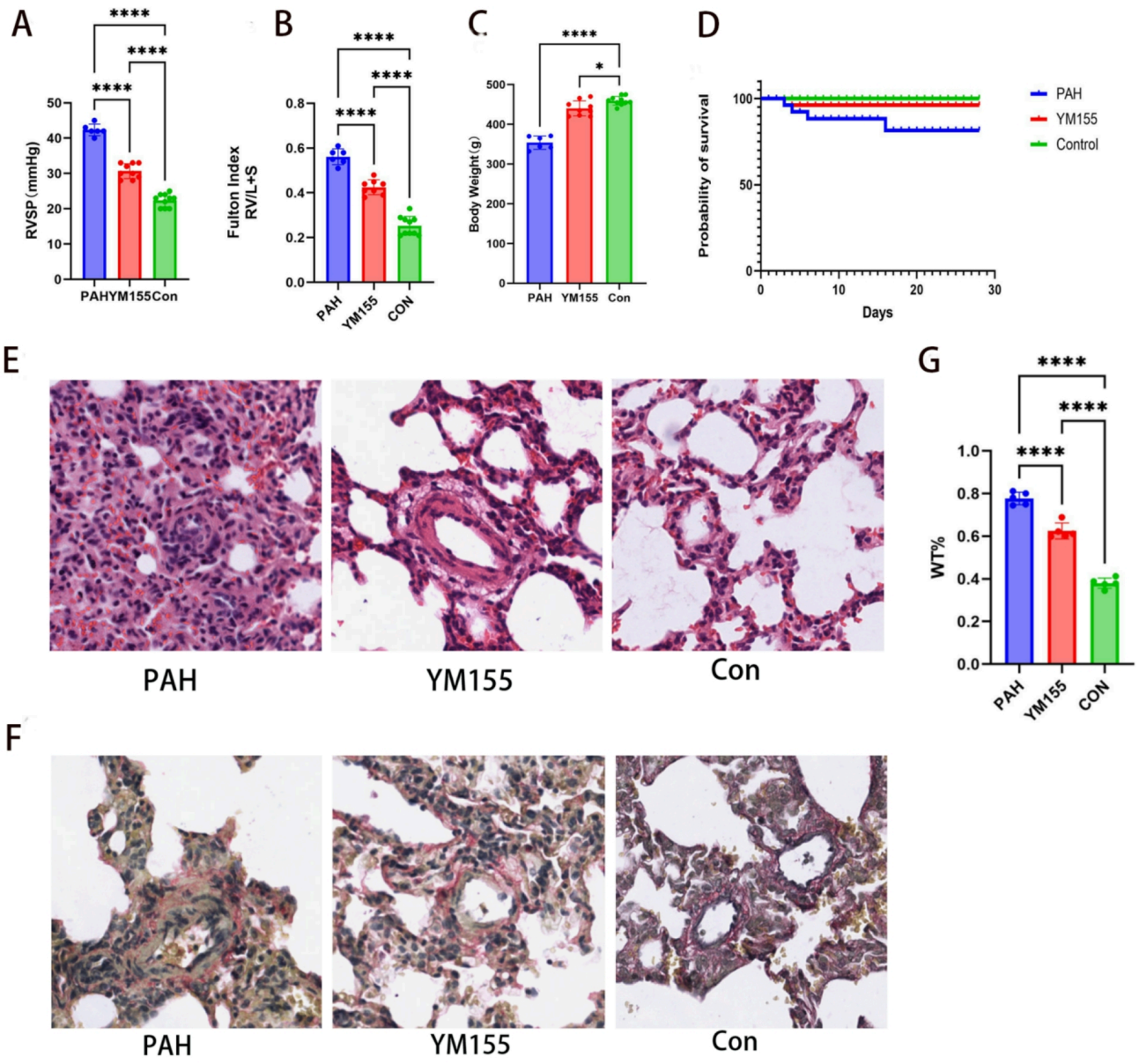

Figure 1

Effect of Survivin on RVSP, Right Ventricular Hypertrophy, Body Weight, and Survival Rate in Rats. (A) Quantitative analysis of right ventricular systolic pressure (RVSP) measured by transthoracic right ventricular puncture. (B) Quantitative analysis of right ventricular hypertrophy assessed by the Fulton index [RV/(LV+S)]. (C) Quantitative analysis of rat body weight at the time of tissue collection. (D) Kaplan-Meier survival curves for rats in each group. (E) Representative images of hematoxylin and eosin (HE) staining showing pulmonary histopathology. (F) Representative images of elastica van Gieson

(EVG) staining showing pulmonary vascular structure. (G) Quantitative analysis of the percentage of pulmonary arteriolar wall thickness (WT%). PAH: pulmonary arterial hypertension model group; YM155: YM155 intervention group; Con: control group. Data are presented as mean ± SD (n = 10 per group). *P < 0.05.

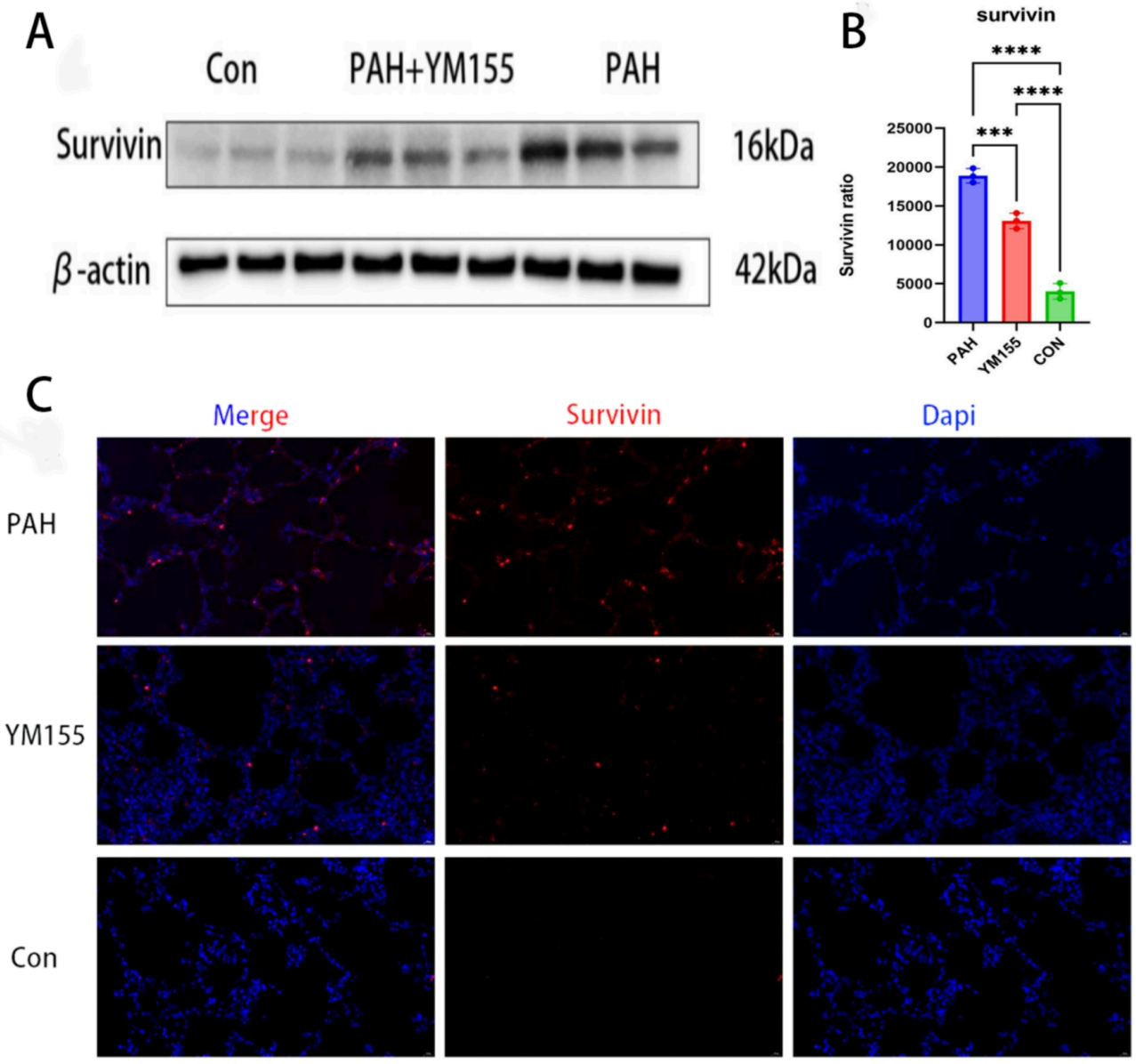

Figure 2

Qualitative and quantitative analysis of Survivin protein expression in rat lung tissue. (A, B) Qualitative and quantitative results of Survivin protein expression in rat lung tissue detected by Western Blot; (C)

Immunofluorescence staining of Survivin in rat lung tissue. PAH: pulmonary hypertension group; YM155: YM155 intervention group; Con: control group; n=10 per group, *p < 0.05.

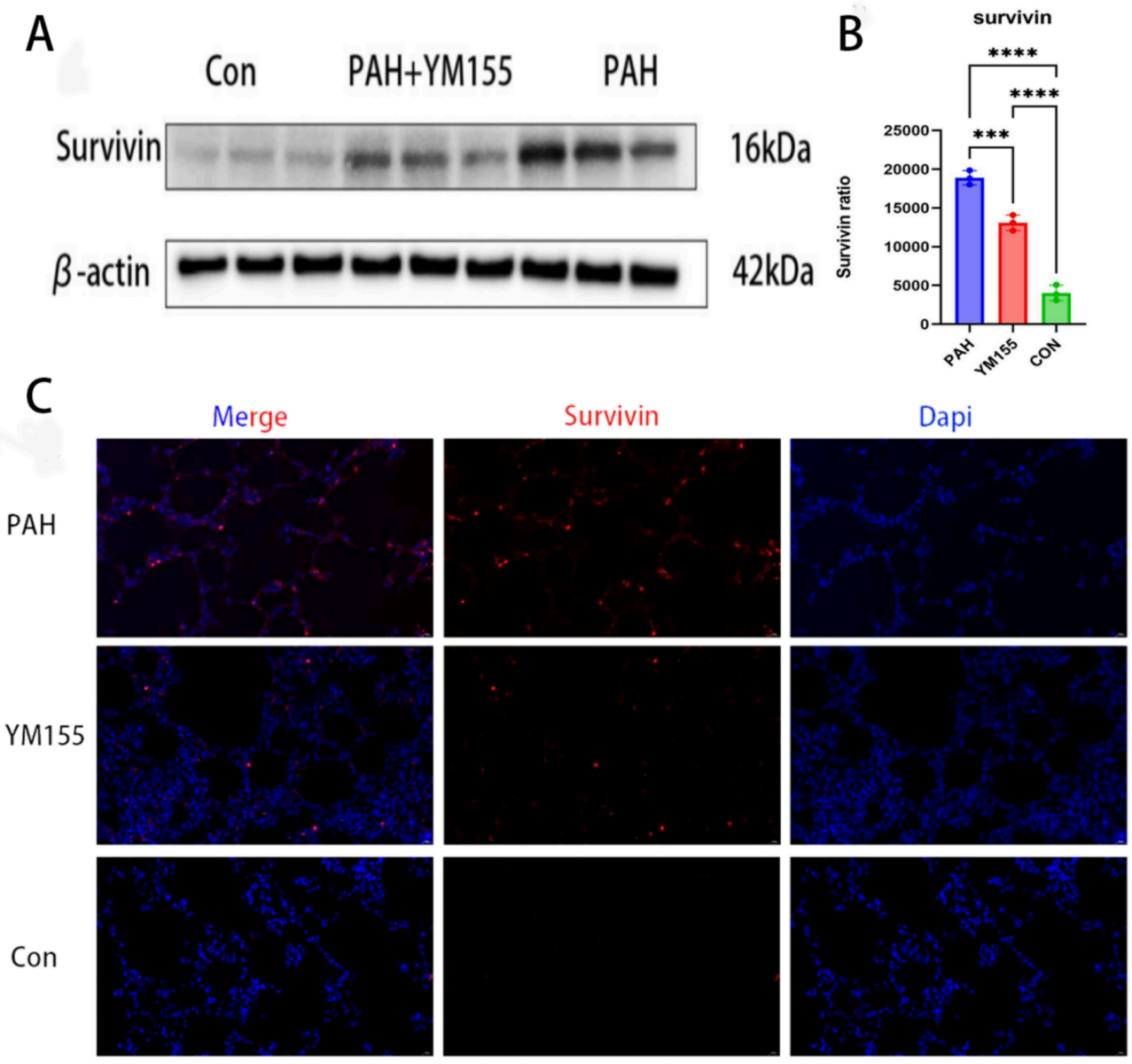

Figure 2

Qualitative and quantitative analysis of Survivin protein expression in rat lung tissue. (A, B) Qualitative and quantitative results of Survivin protein expression in rat lung tissue detected by Western Blot; (C) Immunofluorescence staining of Survivin in rat lung tissue. PAH: pulmonary hypertension group; YM155: YM155 intervention group; Con: control group; n=10 per group, *p < 0.05.

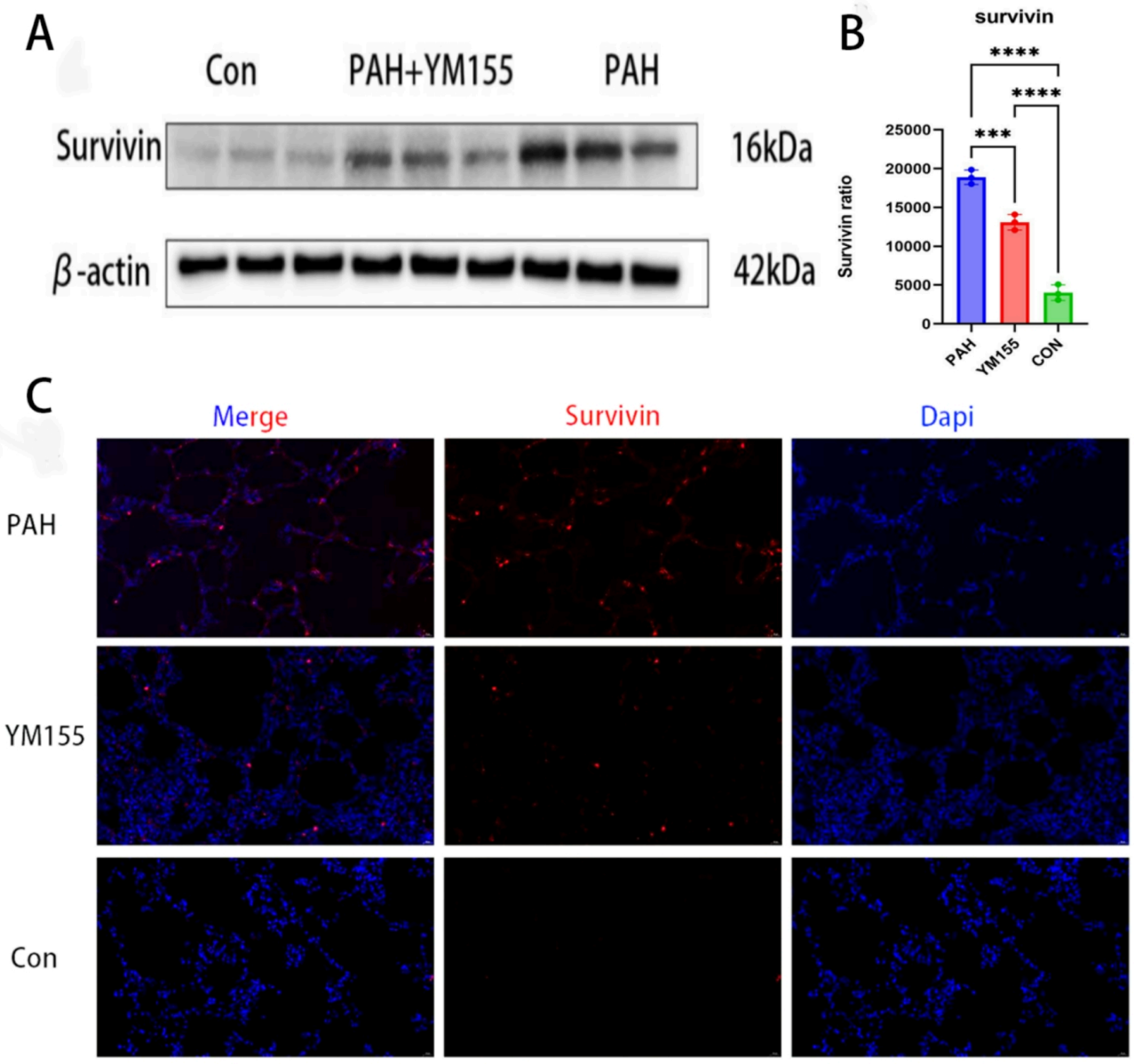

Figure 2

Qualitative and quantitative analysis of Survivin protein expression in rat lung tissue. (A, B) Qualitative and quantitative results of Survivin protein expression in rat lung tissue detected by Western Blot; (C) Immunofluorescence staining of Survivin in rat lung tissue. PAH: pulmonary hypertension group; YM155: YM155 intervention group; Con: control group; n=10 per group, *p < 0.05.

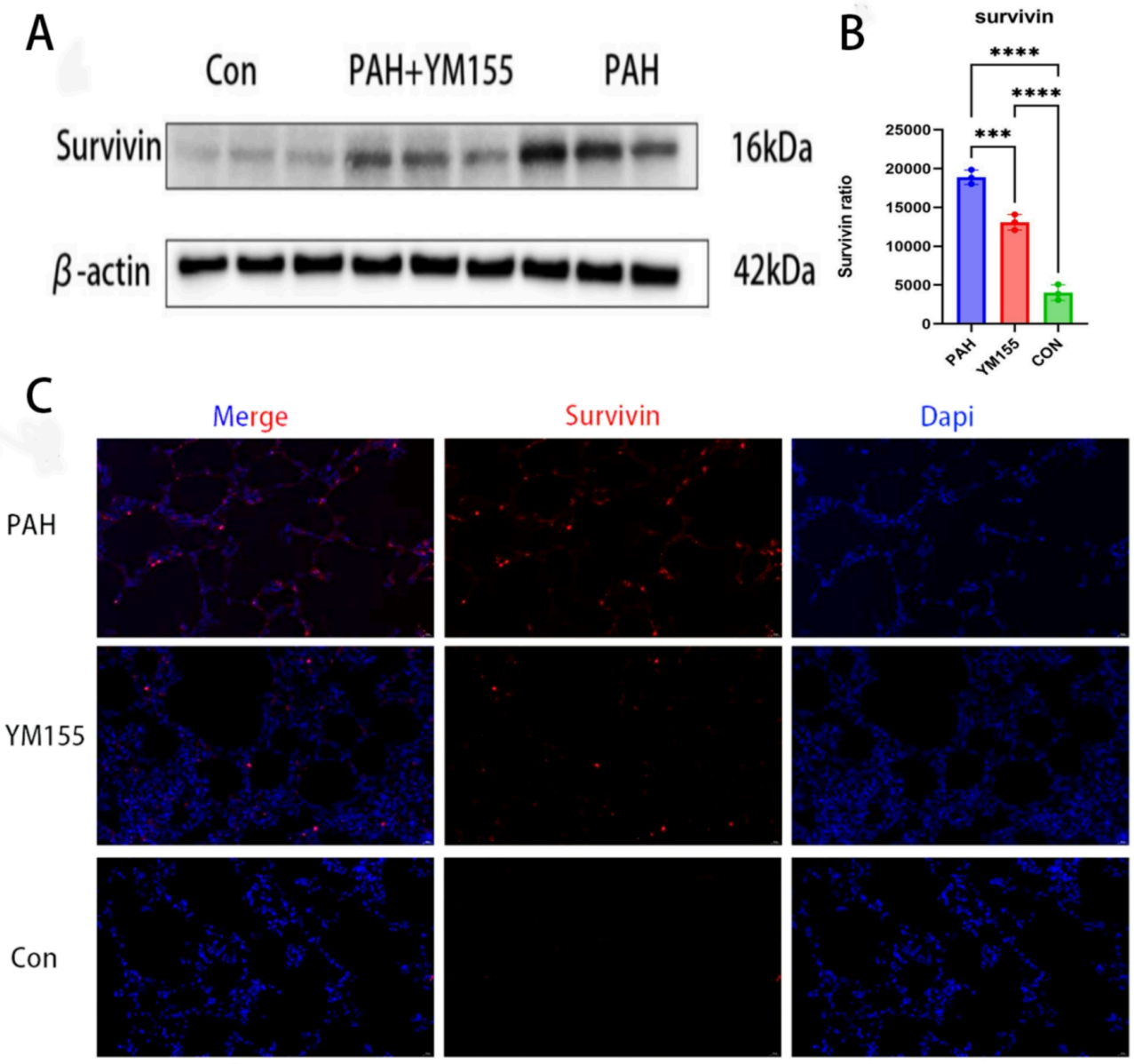

Figure 2

Qualitative and quantitative analysis of Survivin protein expression in rat lung tissue. (A, B) Qualitative and quantitative results of Survivin protein expression in rat lung tissue detected by Western Blot; (C) Immunofluorescence staining of Survivin in rat lung tissue. PAH: pulmonary hypertension group; YM155: YM155 intervention group; Con: control group; n=10 per group, *p < 0.05.

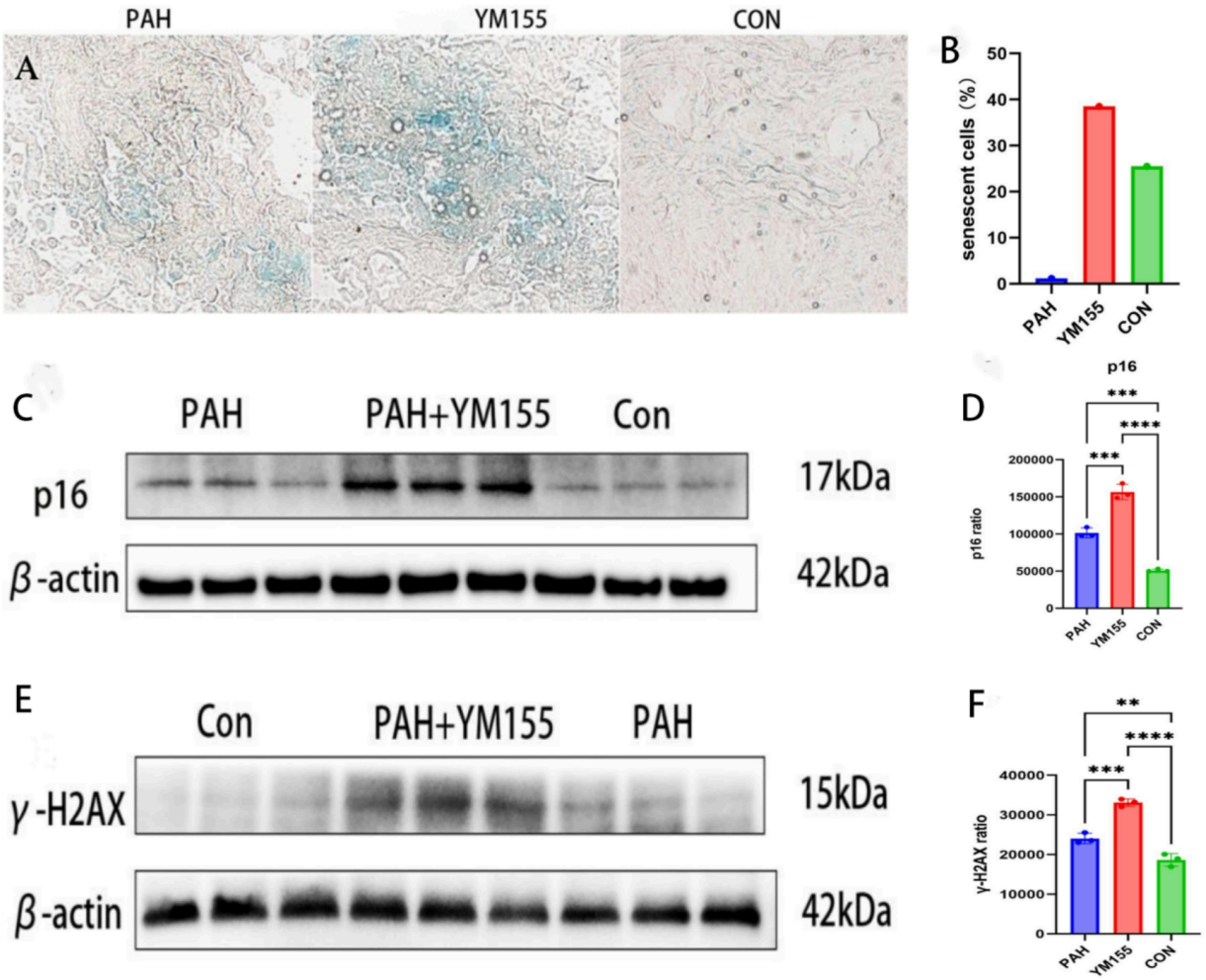

Figure 3

Qualitative and quantitative analysis of cellular senescence-associated indicators. (A) SA-β-Gal staining revealing cellular senescence in lung tissue across different groups; (B) Quantitative analysis of the proportion of senescent cells; (C, D) Representative Western blot bands and quantitative analysis of p16 protein expression; (E, F) Representative Western blot bands and quantitative analysis of γ-H2AX protein expression. PAH: pulmonary hypertension group; YM155: YM155 intervention group; Con: control group; n = 10 per group, $p < 0.05$.

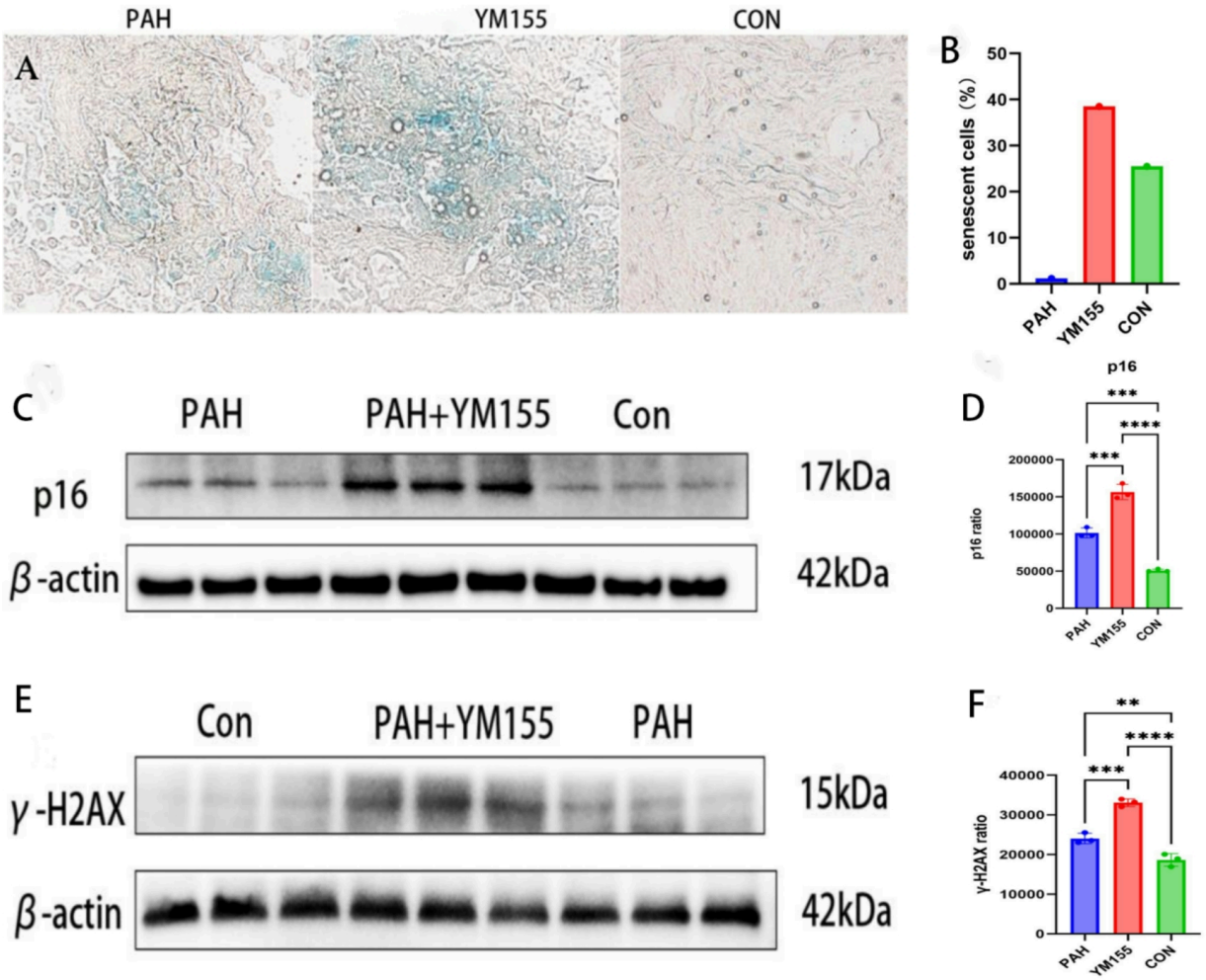

Figure 3

Qualitative and quantitative analysis of cellular senescence-associated indicators. (A) SA-β-Gal staining revealing cellular senescence in lung tissue across different groups; (B) Quantitative analysis of the proportion of senescent cells; (C, D) Representative Western blot bands and quantitative analysis of p16 protein expression; (E, F) Representative Western blot bands and quantitative analysis of γ-H2AX protein expression. PAH: pulmonary hypertension group; YM155: YM155 intervention group; Con: control group; n = 10 per group, $p < 0.05$.

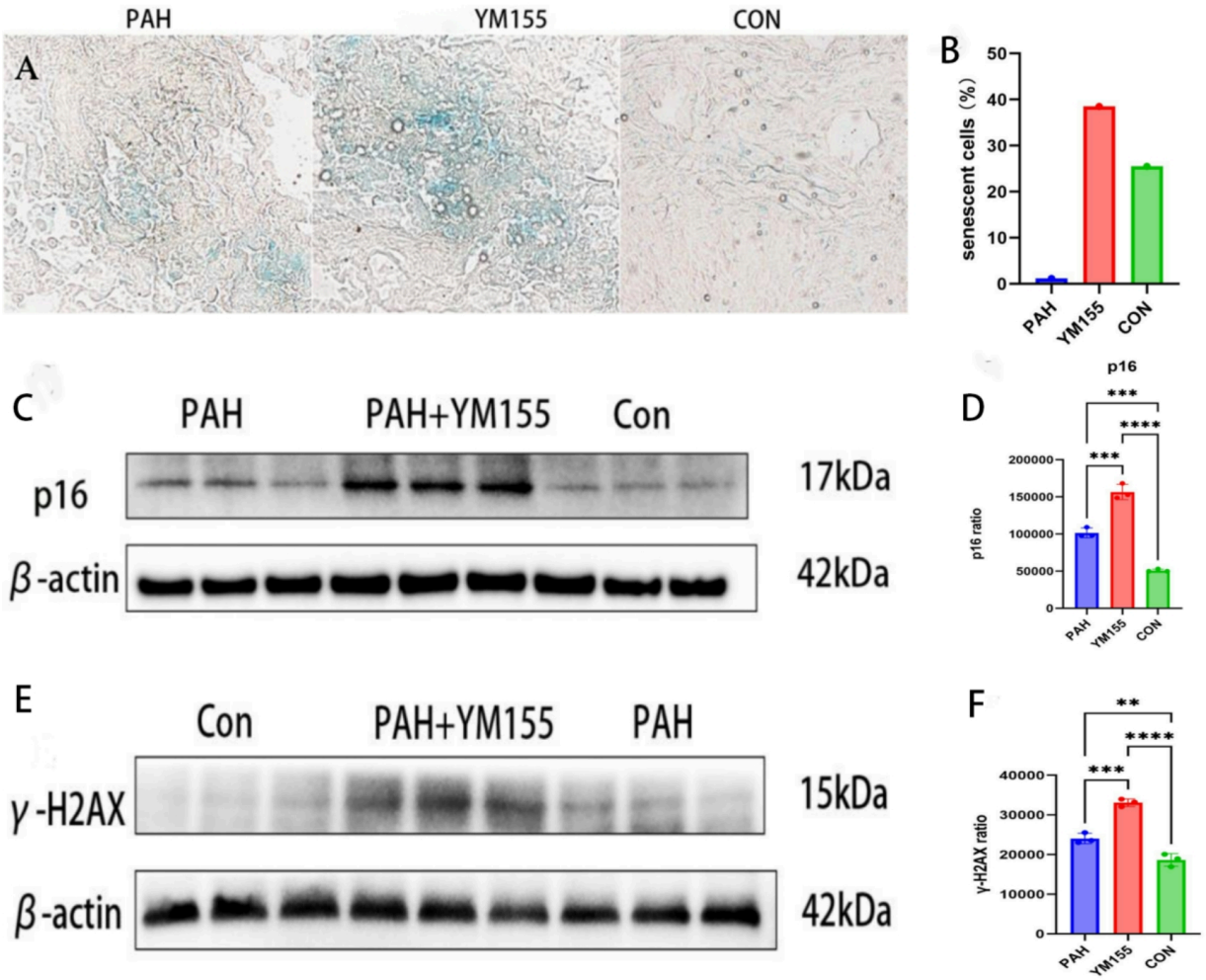

Figure 3

Qualitative and quantitative analysis of cellular senescence-associated indicators. (A) SA-β-Gal staining revealing cellular senescence in lung tissue across different groups; (B) Quantitative analysis of the proportion of senescent cells; (C, D) Representative Western blot bands and quantitative analysis of p16 protein expression; (E, F) Representative Western blot bands and quantitative analysis of γ-H2AX protein expression. PAH: pulmonary hypertension group; YM155: YM155 intervention group; Con: control group; n = 10 per group, $p < 0.05$.

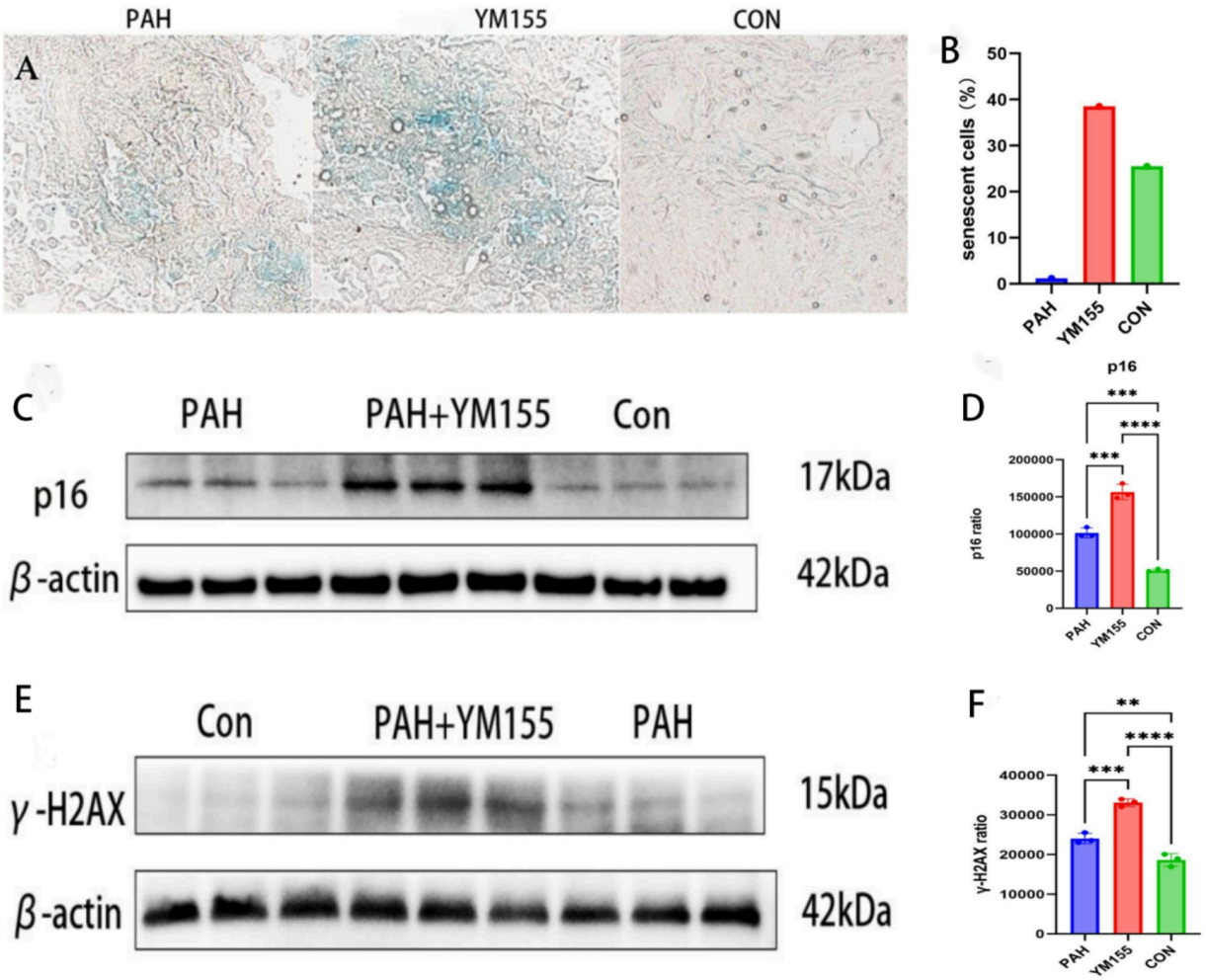

Figure 3

Qualitative and quantitative analysis of cellular senescence-associated indicators. (A) SA-β-Gal staining revealing cellular senescence in lung tissue across different groups; (B) Quantitative analysis of the proportion of senescent cells; (C, D) Representative Western blot bands and quantitative analysis of p16 protein expression; (E, F) Representative Western blot bands and quantitative analysis of γ-H2AX protein expression. PAH: pulmonary hypertension group; YM155: YM155 intervention group; Con: control group; n = 10 per group, $p < 0.05$.

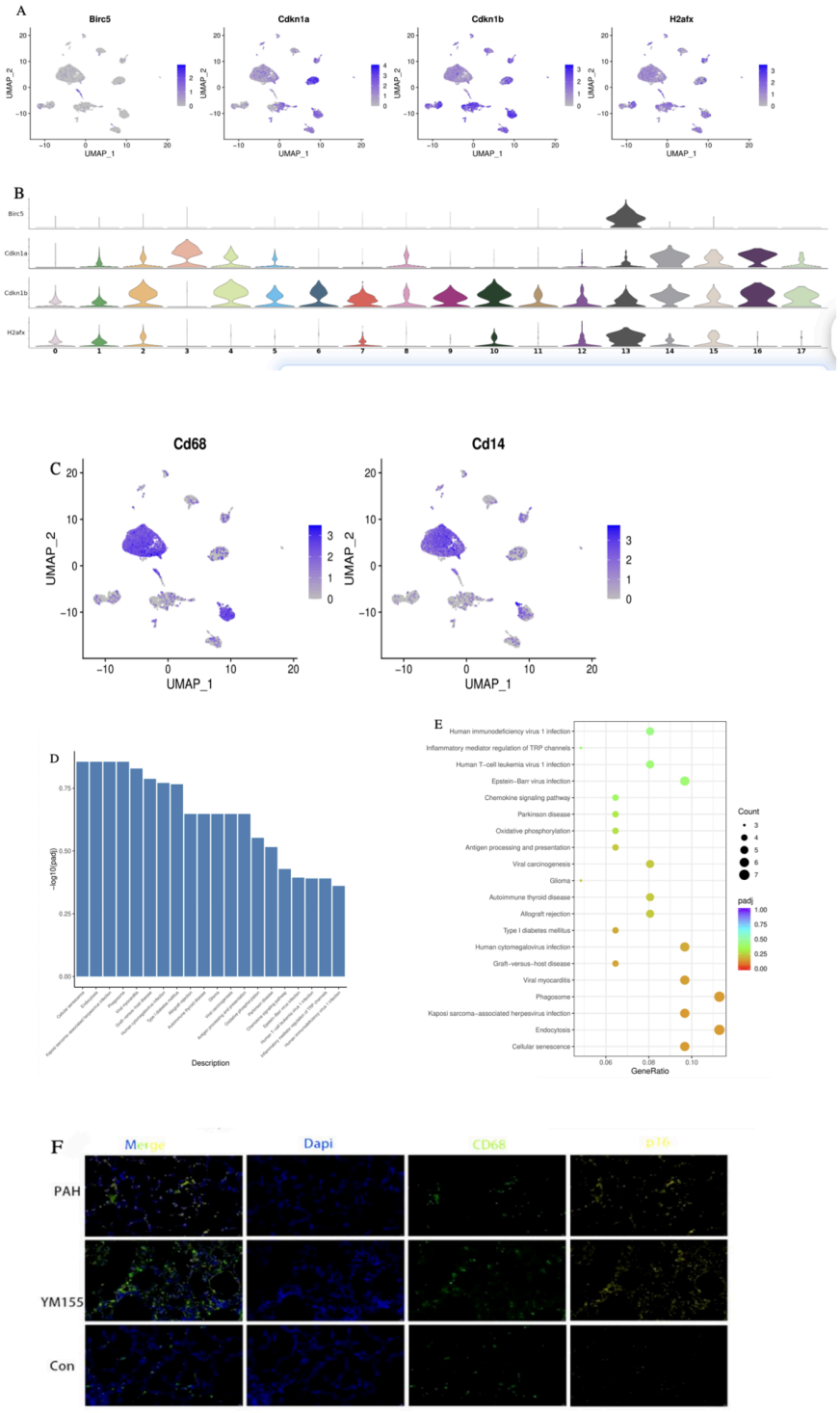

Figure 4

Cellular localization analysis of Survivin and senescence-associated markers. (A, B, C) Expression distribution of Birc5 (the gene encoding Survivin) in the cellular atlas, showing its high expression in the macrophage cluster. Upregulation of senescence-associated markers Cdkn2a (p16) and Cdkn1a (p21), as well as the DNA damage marker H2afx (γ-H2AX), in the macrophage cluster. (D, E) KEGG pathway enrichment analysis of the top 50 upregulated genes in the PAH group, showing significant enrichment

of cellular senescence and cell cycle-related pathways. (F) Co-immunofluorescence staining for CD68 (a macrophage marker) and p16, further validating the expression of senescence markers in macrophages at the protein level.

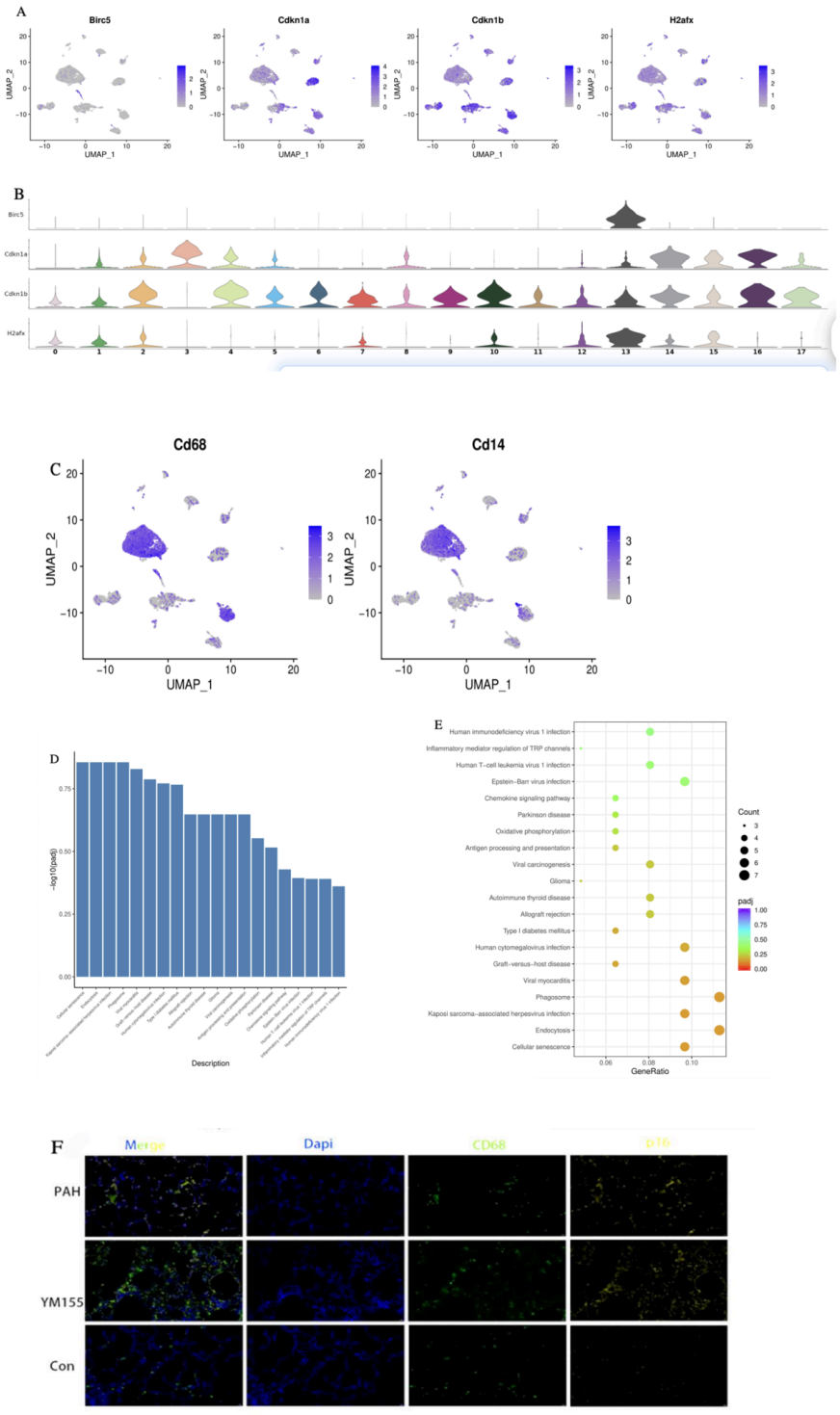

Figure 4

Cellular localization analysis of Survivin and senescence-associated markers. (A, B, C) Expression distribution of Birc5 (the gene encoding Survivin) in the cellular atlas, showing its high expression in the macrophage cluster. Upregulation of senescence-associated markers Cdkn2a (p16) and Cdkn1a (p21), as well as the DNA damage marker H2afx (γ-H2AX), in the macrophage cluster. (D, E) KEGG pathway enrichment analysis of the top 50 upregulated genes in the PAH group, showing significant enrichment of cellular senescence and cell cycle-related pathways. (F) Co-immunofluorescence staining for CD68 (a macrophage marker) and p16, further validating the expression of senescence markers in macrophages at the protein level.

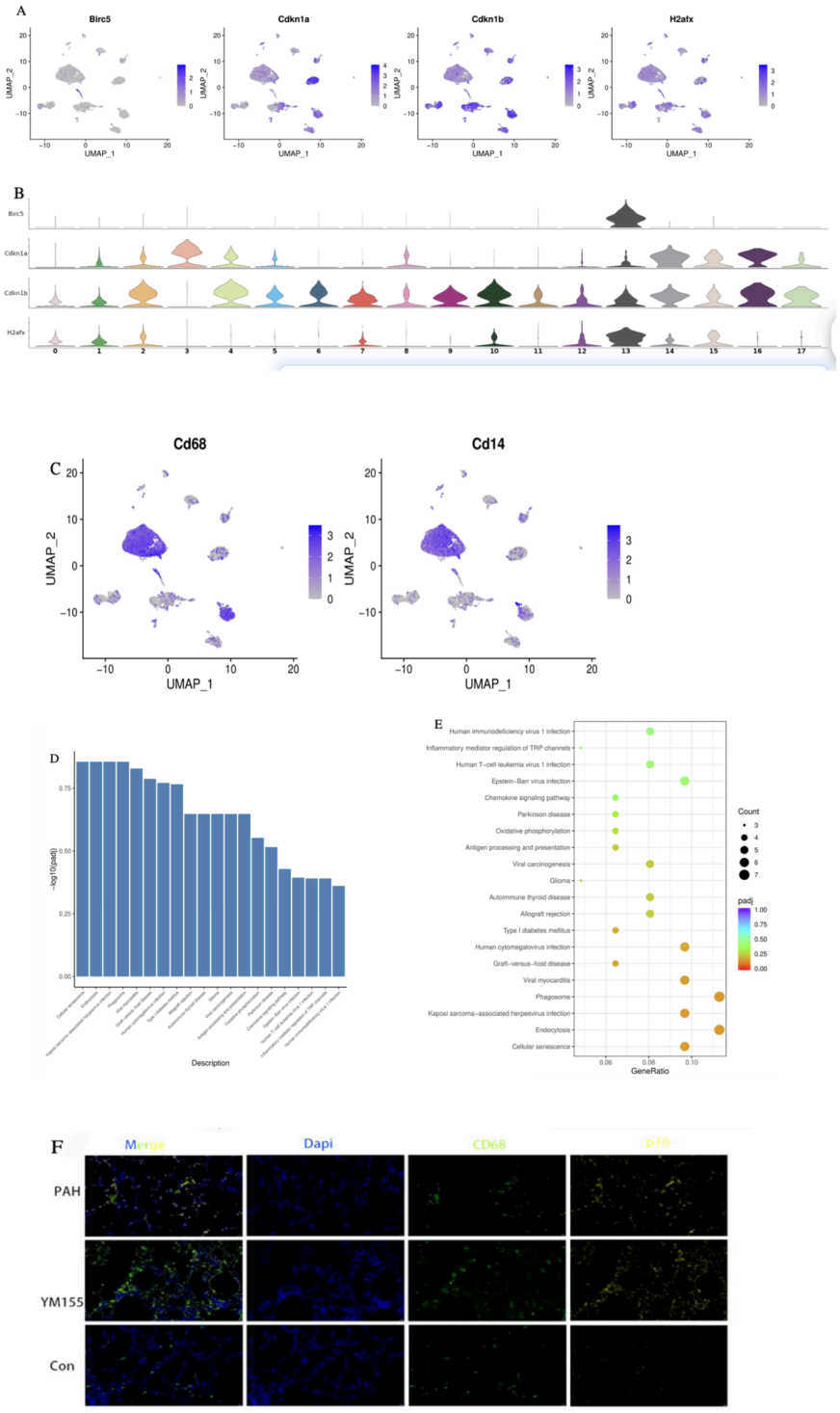

Figure 4

Cellular localization analysis of Survivin and senescence-associated markers. (A, B, C) Expression distribution of Birc5 (the gene encoding Survivin) in the cellular atlas, showing its high expression in the macrophage cluster. Upregulation of senescence-associated markers Cdkn2a (p16) and Cdkn1a (p21), as well as the DNA damage marker H2afx (γ-H2AX), in the macrophage cluster. (D, E) KEGG pathway enrichment analysis of the top 50 upregulated genes in the PAH group, showing significant enrichment

of cellular senescence and cell cycle-related pathways. (F) Co-immunofluorescence staining for CD68 (a macrophage marker) and p16, further validating the expression of senescence markers in macrophages at the protein level.

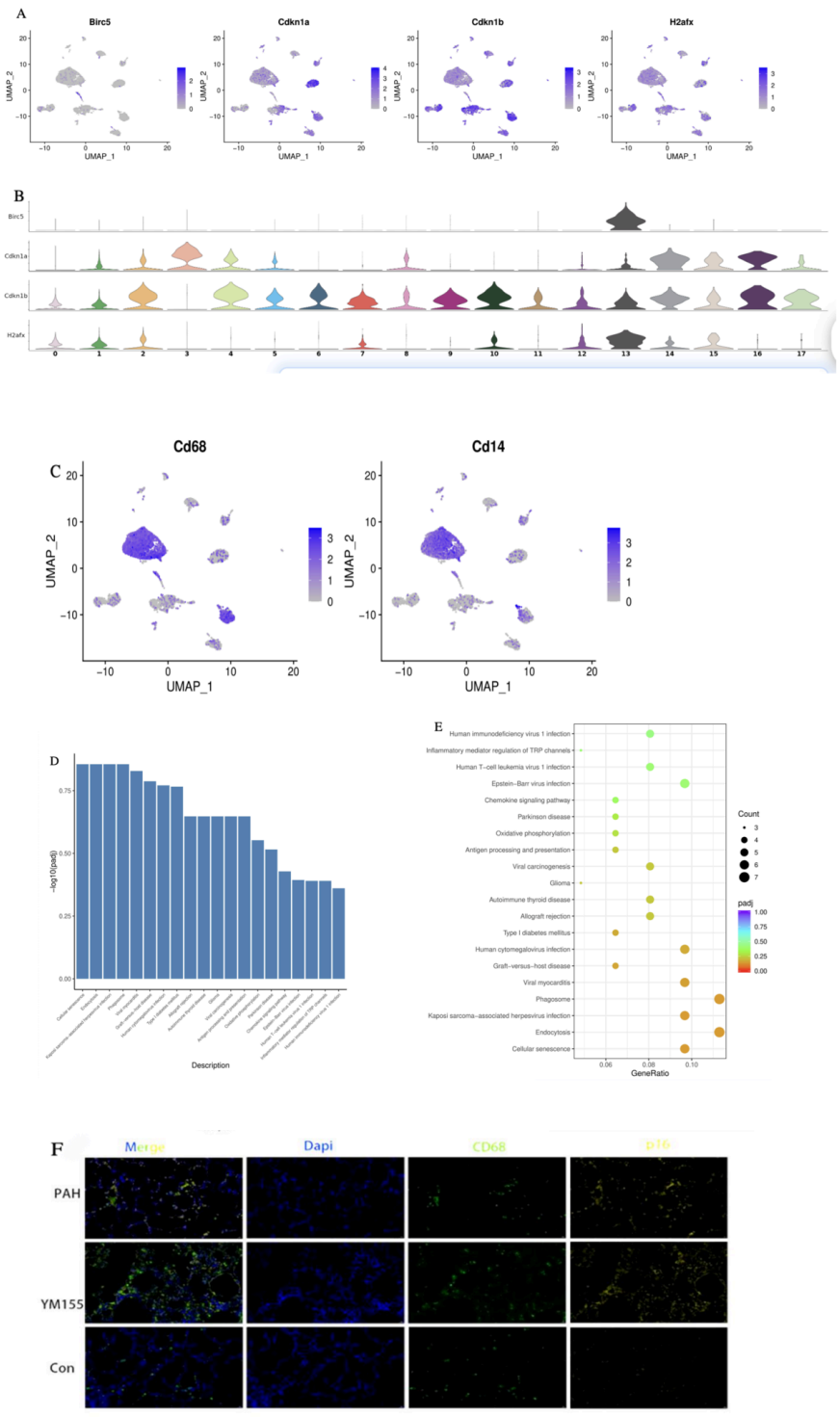

Figure 4

Cellular localization analysis of Survivin and senescence-associated markers. (A, B, C) Expression distribution of Birc5 (the gene encoding Survivin) in the cellular atlas, showing its high expression in the macrophage cluster. Upregulation of senescence-associated markers Cdkn2a (p16) and Cdkn1a (p21), as well as the DNA damage marker H2afx (γ-H2AX), in the macrophage cluster. (D, E) KEGG pathway enrichment analysis of the top 50 upregulated genes in the PAH group, showing significant enrichment of cellular senescence and cell cycle-related pathways. (F) Co-immunofluorescence staining for CD68 (a macrophage marker) and p16, further validating the expression of senescence markers in macrophages at the protein level.

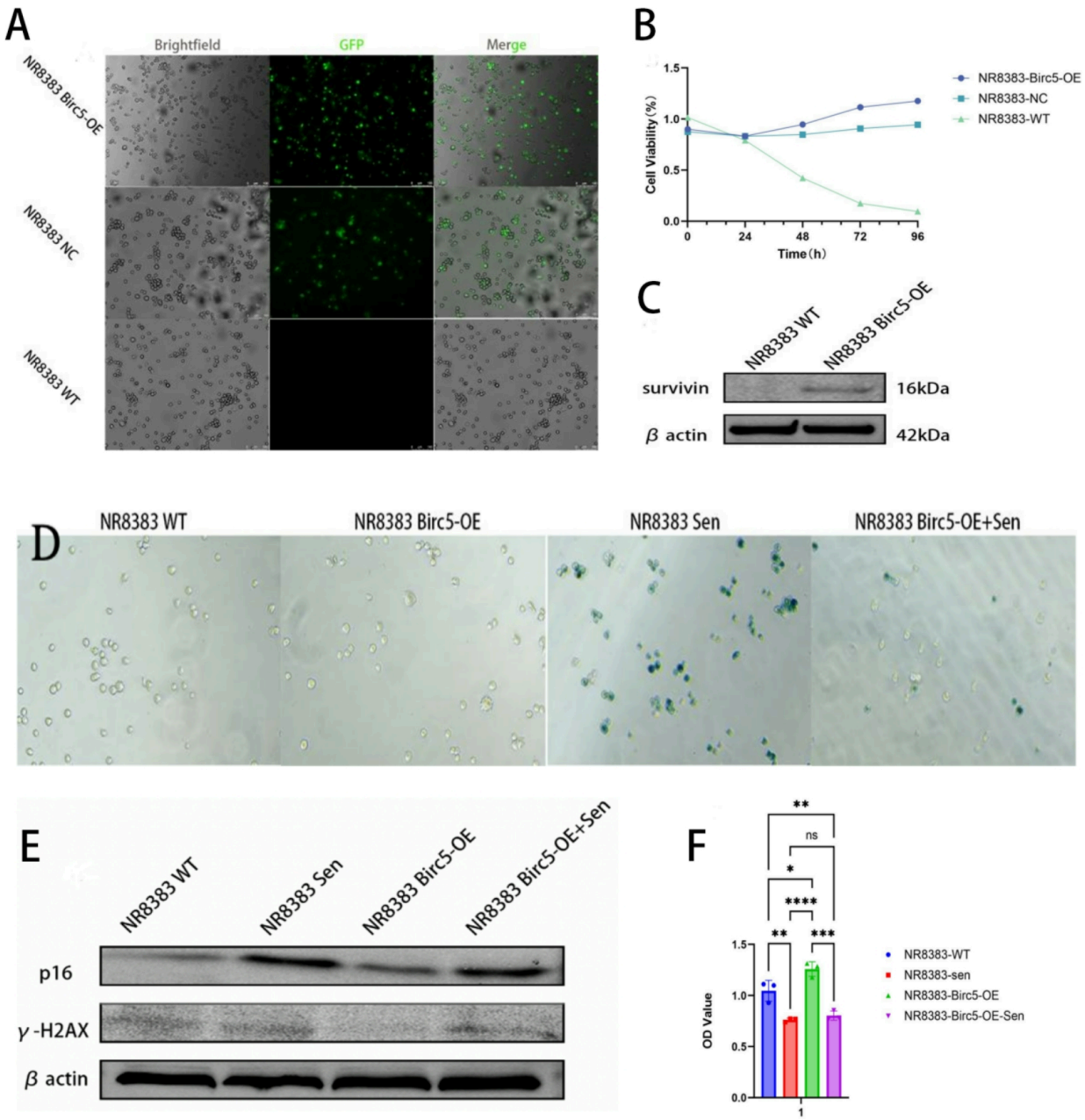

Figure 5

In vitro validation of the association between Survivin and cellular senescence through Birc5 overexpression.(A) Fluorescence microscopy images of NR8383 cells 48 hours post-lentiviral transduction, demonstrating successful transduction and expression of the GFP reporter gene. (B) CCK-8 assay monitoring cell viability during puromycin selection. The viability of wild-type (WT) cells declined sharply, whereas NC and Birc5-OE groups maintained stable viability, confirming successful establishment of stable transgenic cell lines. (C) Western blot analysis confirming successful introduction and stable expression of the Birc5 gene in NR8383 cells. (D) SA-β-Gal staining for detecting cellular senescence. Following doxorubicin induction, a large number of senescent cells were observed in the senescence (Sen) group, while the number of positive cells was significantly reduced in the Birc5-OE+Sen group. (E) Western blot analysis of p16 and γ-H2AX protein expression. Doxorubicin induction increased p16 and γ-H2AX expression in the Sen group, whereas expression levels were reduced in the Birc5-OE+Sen group, indicating that Survivin overexpression attenuates cellular senescence and DNA damage. (F) CCK-8 assay following co-culture of NR8383 cells with pulmonary arterial smooth muscle cells (PASMCs), demonstrating that senescent NR8383 cells inhibit the proliferation of surrounding PASMCs.

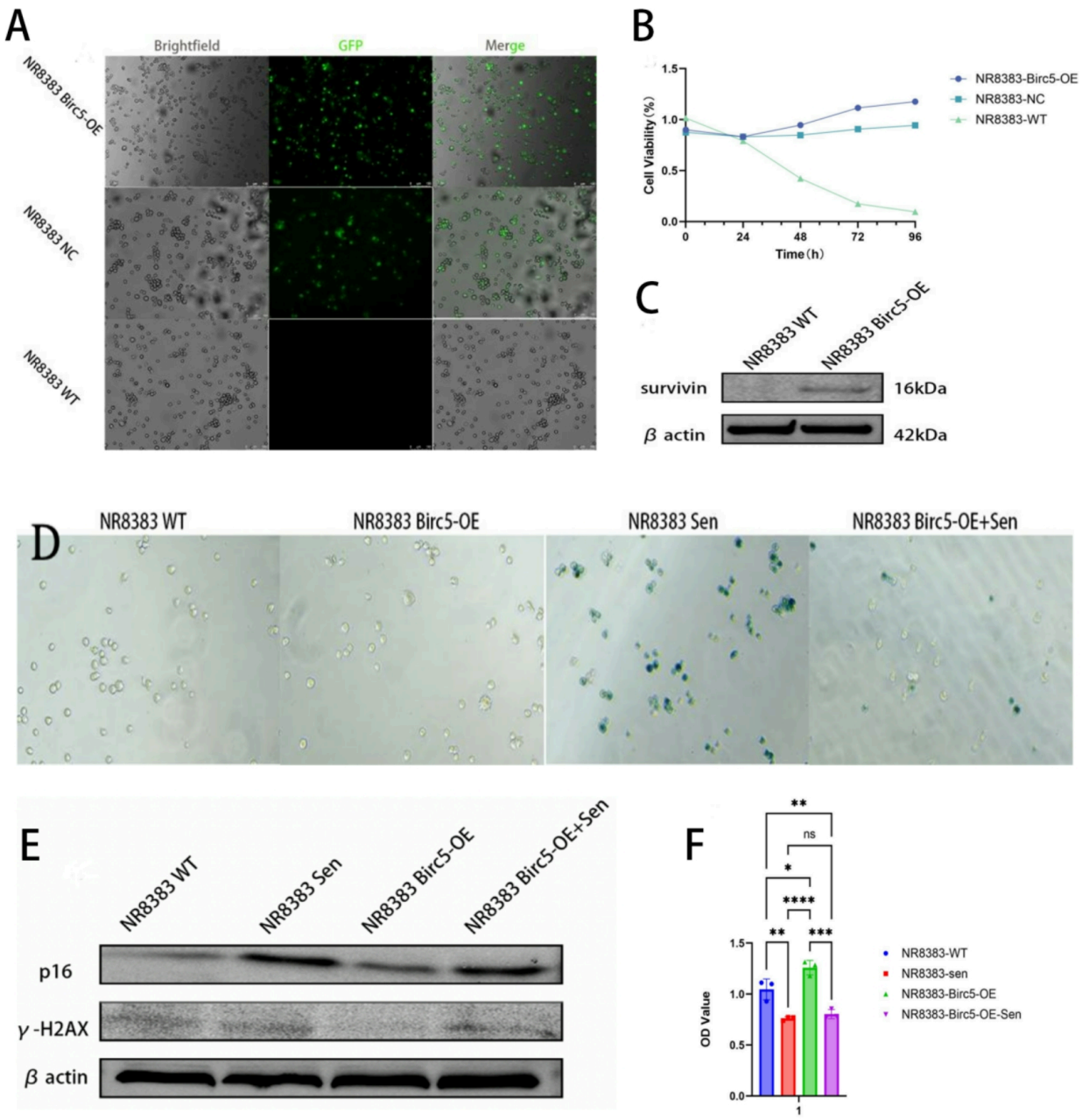

Figure 5

In vitro validation of the association between Survivin and cellular senescence through Birc5 overexpression.(A) Fluorescence microscopy images of NR8383 cells 48 hours post-lentiviral transduction, demonstrating successful transduction and expression of the GFP reporter gene. (B) CCK-8 assay monitoring cell viability during puromycin selection. The viability of wild-type (WT) cells declined sharply, whereas NC and Birc5-OE groups maintained stable viability, confirming successful establishment of stable transgenic cell lines. (C) Western blot analysis confirming successful introduction and stable expression of the Birc5 gene in NR8383 cells. (D) SA-β-Gal staining for detecting

cellular senescence. Following doxorubicin induction, a large number of senescent cells were observed in the senescence (Sen) group, while the number of positive cells was significantly reduced in the Birc5-OE+Sen group. (E) Western blot analysis of p16 and γ-H2AX protein expression. Doxorubicin induction increased p16 and γ-H2AX expression in the Sen group, whereas expression levels were reduced in the Birc5-OE+Sen group, indicating that Survivin overexpression attenuates cellular senescence and DNA damage. (F) CCK-8 assay following co-culture of NR8383 cells with pulmonary arterial smooth muscle cells (PASMCs), demonstrating that senescent NR8383 cells inhibit the proliferation of surrounding PASMCs.

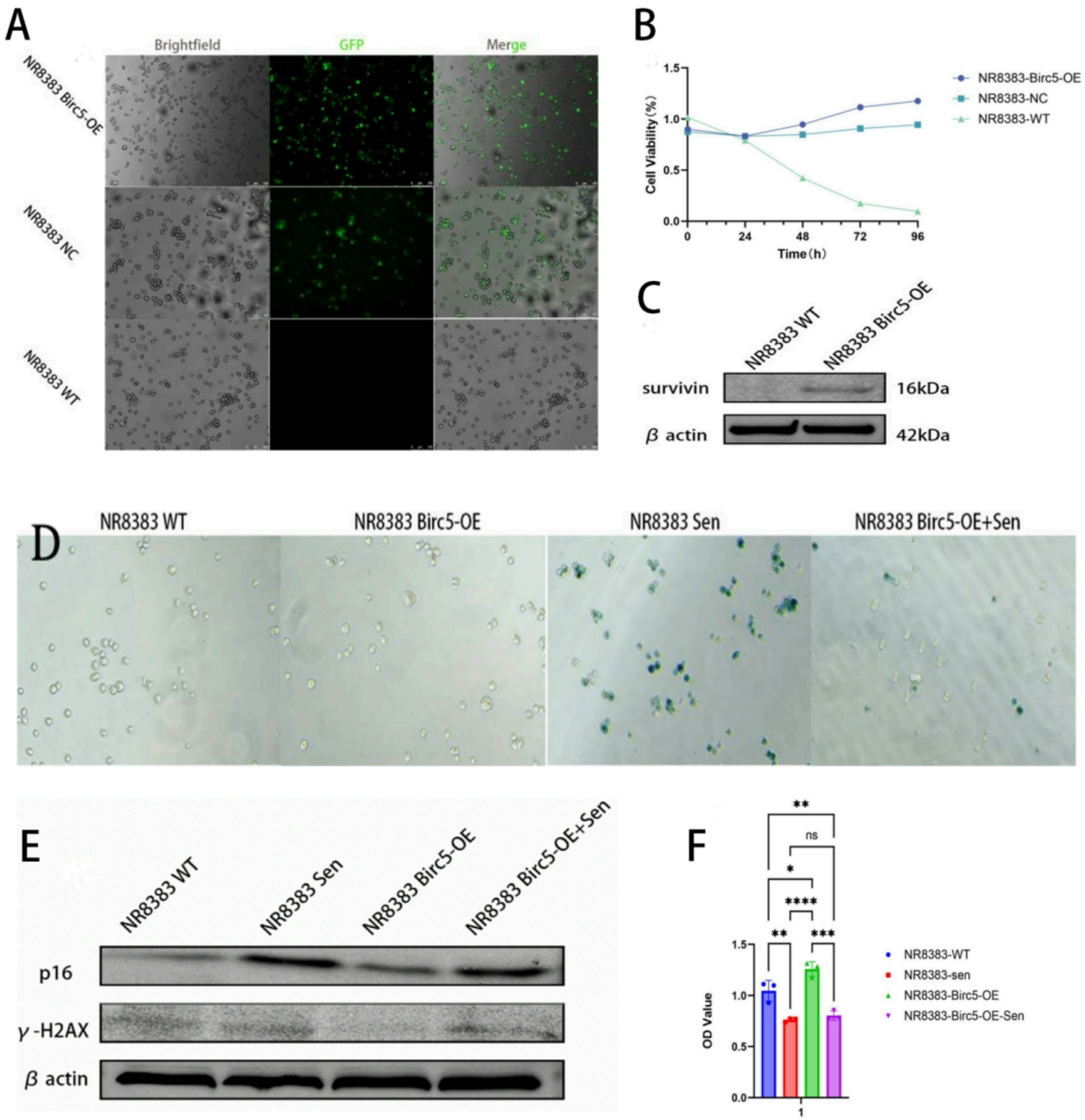

Figure 5

In vitro validation of the association between Survivin and cellular senescence through Birc5 overexpression.(A) Fluorescence microscopy images of NR8383 cells 48 hours post-lentiviral transduction, demonstrating successful transduction and expression of the GFP reporter gene. (B) CCK-8 assay monitoring cell viability during puromycin selection. The viability of wild-type (WT) cells declined sharply, whereas NC and Birc5-OE groups maintained stable viability, confirming successful establishment of stable transgenic cell lines. (C) Western blot analysis confirming successful introduction and stable expression of the Birc5 gene in NR8383 cells. (D) SA-β-Gal staining for detecting cellular senescence. Following doxorubicin induction, a large number of senescent cells were observed in the senescence (Sen) group, while the number of positive cells was significantly reduced in the Birc5-OE+Sen group. (E) Western blot analysis of p16 and γ-H2AX protein expression. Doxorubicin induction increased p16 and γ-H2AX expression in the Sen group, whereas expression levels were reduced in the Birc5-OE+Sen group, indicating that Survivin overexpression attenuates cellular senescence and DNA damage. (F) CCK-8 assay following co-culture of NR8383 cells with pulmonary arterial smooth muscle cells (PASMCs), demonstrating that senescent NR8383 cells inhibit the proliferation of surrounding PASMCs.

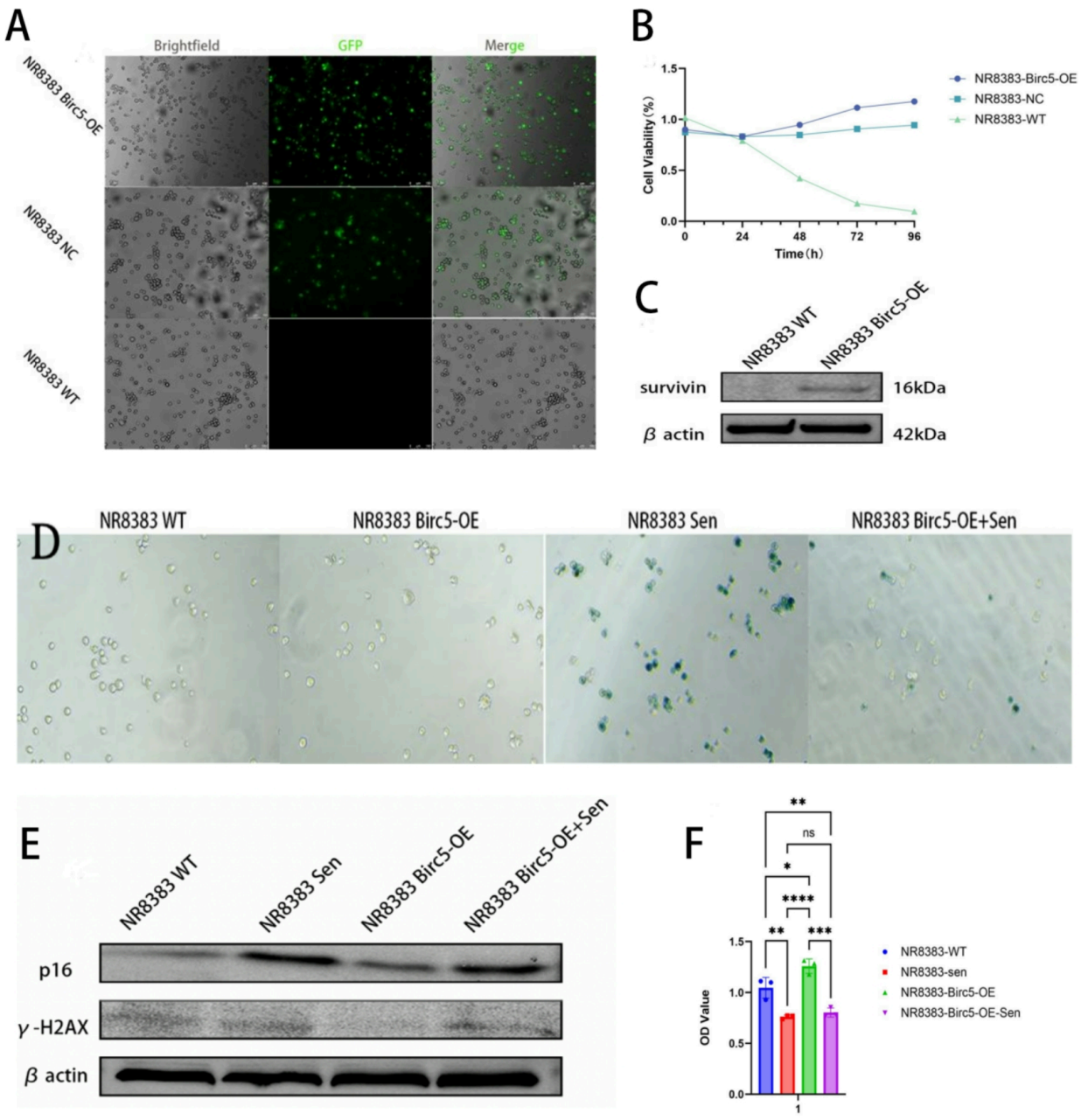

Figure 5

In vitro validation of the association between Survivin and cellular senescence through Birc5 overexpression.(A) Fluorescence microscopy images of NR8383 cells 48 hours post-lentiviral transduction, demonstrating successful transduction and expression of the GFP reporter gene. (B) CCK-8 assay monitoring cell viability during puromycin selection. The viability of wild-type (WT) cells declined sharply, whereas NC and Birc5-OE groups maintained stable viability, confirming successful establishment of stable transgenic cell lines. (C) Western blot analysis confirming successful introduction and stable expression of the Birc5 gene in NR8383 cells. (D) SA-β-Gal staining for detecting

cellular senescence. Following doxorubicin induction, a large number of senescent cells were observed in the senescence (Sen) group, while the number of positive cells was significantly reduced in the Birc5-OE+Sen group. (E) Western blot analysis of p16 and γ-H2AX protein expression. Doxorubicin induction increased p16 and γ-H2AX expression in the Sen group, whereas expression levels were reduced in the Birc5-OE+Sen group, indicating that Survivin overexpression attenuates cellular senescence and DNA damage. (F) CCK-8 assay following co-culture of NR8383 cells with pulmonary arterial smooth muscle cells (PASMCs), demonstrating that senescent NR8383 cells inhibit the proliferation of surrounding PASMCs.

Supplementary Files

This is a list of supplementary files associated with this preprint. Click to download.

- SupplementaryInformation.pdfd1.pdf
- SupplementaryInformation.pdfd1.pdf
- SupplementaryInformation.pdfd1.pdf
- SupplementaryInformation.pdfd1.pdf